FOUR-WAVE MIXING BELOW ROOM

TEMPERATURE IN Eu^{3+} DOPED

SILICATE GLASSES

By

JASON A. PAXTON

Bachelor of Science

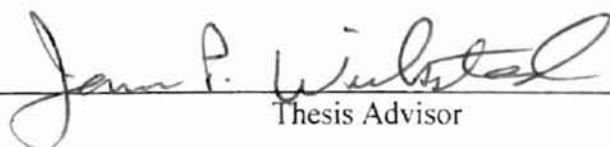University of Central Oklahoma

Edmond, Oklahoma

1997

Submitted to the Faculty of the
Graduate College of the
Oklahoma State University
in partial fulfillment of
the requirements for
the Degree of
MASTER OF SCIENCE
December, 1999

FOUR-WAVE MIXING BELOW ROOM

TEMPERATURE IN Eu^{3+} DOPED

SILICATE GLASSES

Thesis Approved:

_____

Thesis Advisor

_____

_____

Waype B. Porwell

Dean of the Graduate College

ii

Acknowledgements

I would like to express thanks to my advisor, Dr. James Wicksted, whose insight and guidance were invaluable to the completion of this thesis. I would also like to thank my thesis committee members, Dr. George Dixon, and Dr. Joel Martin for helping to steer me in the right direction so many times. Special thanks go to Dr. Abdullatif Hamad for all that he taught me during our work together in the lab. Also, many thanks go to Dr. Joel Martin for the design and construction of the dewar used in the experiments, and to Charles Hunt for batching the glass samples.

I want to express gratitude to my family, especially my mother and father, for their love and support, not just during my graduate work, but throughout my whole life. Also, I want to thank Jennifer, my soon-to-be wife, for taking care of all of our wedding preparations while I finished this thesis.

TABLE OF CONTENTS

LIST OF TABLES

LIST OF FIGURES

CHAPTER I

INTRODUCTION

Four-Wave Mixing at Room Temperature

The formation of laser-induced permanent and transient refractive index gratings in Eu^{3+} doped silicate glasses has been well documented [1-10]. Typically these laser-induced gratings (LIG) are formed at room temperature by intersecting two laser beams (write-beams) inside a glass sample to form an interference pattern. The modulated intensity of the interference pattern modulates the optical properties of the sample to produce the refractive index grating.

The transient component of the LIG has been shown to be due to a spatial variation of the population of excited Eu^{3+} rare-earth modifiers [3], which are resonantly excited to the $^5D_2$ level and relax non-radiatively to the $^5D_0$ metastable state.

Two models have been proposed to explain the mechanism involved in the formation of the permanent LIG. A tunneling model was proposed by Behrens *et al.* [3] in which the network former and modifier ions of the glass host can arrange themselves into two different configurations in the local environment of the Eu^{3+} ions. The assumption is that each configuration produces a different index of refraction. Behrens proposes that the energy to initiate the move from one equilibrium

configuration to another is produced by the high-energy phonons created through the non-radiative relaxation of the Eu^{3+} ions from the $^5D_2$ level to the $^5D_0$ level. The local heating of these vibrational modes is the cause of the change in structure around the Eu^{3+} ions.

More recently, Dixon *et al.* proposed that long-range migration of small modifiers away from the illuminated regions of the write beams was the mechanism involved in permanent grating formation [11]. The energy necessary for the migration was again attributed to the high-energy phonons produced from the non-radiative relaxation of Eu^{3+} ions.

Understanding the mechanism by which permanent LIG are formed is important due to the potential device applications of glasses that maintain a permanent grating. Examples of such devices are holographic storage devices and holographic narrow-band rejection filters (notch filters) that can be used as channel selectors for wavelength-multiplexed optical fiber systems [1].

Obviously, a strong grating efficiency is desirable in these devices, and the need for new methods of forming stronger LIG in glasses using four-wave mixing (FWM) techniques is apparent. LIG formation below room temperature has shown potential for increased grating efficiency [3,5] and will be the topic of this thesis.

Four-Wave Mixing Below Room Temperature

Few studies on the effects of low temperature on LIG formation in Eu^{3+} doped glasses have been reported to date. French *et al.* [5] reported results of measurements

of LIG signal intensity in Eu^{3+} doped silicate glasses at temperatures below room temperature and found a trend toward increased LIG signal intensity as temperature was lowered. This trend was reported for the temperature range 160K to 380K. Behrens *et al.* [3] reported results in the range 160K to 300K in Eu^{3+} doped phosphate glasses, and discovered the same trend. Both authors used the tunneling model to explain the temperature dependence in diffracted signal intensity.

From the descriptions given by French *et al.* [5] and Behrens *et al.* [3], the point at which the scattering efficiency from the permanent LIG was measured is unclear. In the FWM experiments reported in this thesis, it was found that in certain cases during grating formation, there is an initial maximum in the diffracted signal followed by a minimum and then a large monotonic increase. The increase in the diffracted signal after the minimum was seen to be anywhere from 0.5 to 19 times the initial maximum depending on several parameters including temperature and write time. It was also found that when the write beams were turned off, the grating strength continued to increase resulting in a diffracted power up to 164 times the initial maximum. Thus it was found that the point in the LIG formation process at which the scattering efficiency is measured is important in characterizing the LIG.

The purpose of this thesis is to present new results of FWM experiments conducted below room temperature and to give a qualitative description of the mechanisms involved in the production of LIG. In addition, it will be shown that stronger permanent gratings can be formed below room temperature with up to 95% of the grating remaining at room temperature depending on the exact grating formation process and sample composition.

CHAPTER II

EXPERIMENT

Sample Composition and Preparation

Two samples were used for the experiments reported in this thesis, and the composition of each sample is given by the following:

$$[70\ SiO_2 + 15\ Na_2O + 12\ MgO + 3\ Al_2O_3](1 - x) : xEu_2O_3,$$

where $x = 2.5$ and 5 in mole%. Each sample will be referred to by its Eu_2O_3 mole percentage. Glass compositions were formed from europium carbonate, aluminum hydroxide, alkali carbonate, alkaline earth carbonate, and silica precursor powders. All powders were mixed in a mixer for approximately one hour before being transferred to a platinum crucible. To melt the powders, the crucible was placed in a melting furnace at 1650^0C for 8-50 hours, after which the charged crucible was cooled to 1550^0C at $-10^0C/hr$ during the melting furnace ramp-down. The crucible and charge were then placed in a separate annealing oven (pre-heated to $450-550^0C$) and annealed for 1 hour at $700-725^0C$. A core drill was used to remove the annealed glass from the crucible, and the glass was then cut to a rectangular shape with dimensions listed in Table I. The sample faces were then ground and polished to optical quality using cerium oxide polishing compound.

Experimental Setup

The experimental setup is shown in Figure 1. The typical non-degenerate FWM technique was used to detect the first-order Bragg diffraction from LIG in the Eu2.5 and Eu5 samples. The experiments were conducted at three temperatures: 298K, 265K, and 238K, and these were kept constant to within 1K. To maintain a sample at a lower temperature, it was placed in a cube shaped thermoelectric cryostat with a circular window on each side. Entrance and exit windows were BK7 glass with an anti-reflection coating to minimize the loss of power from write, read, and diffracted beams. The thermoelectric cryostat dimensions were approximately 3 x 3 x 4 inches, and the windows each had a diameter of 2 inches. A Melcor multistage thermoelectric cooler was attached to the lid of the thermoelectric cryostat so that it was contained inside when the lid was closed. Copper plates extended from the thermoelectric cooler, which were used to hold and transfer heat from the sample. A heat sink and fan were attached to the outer part of the thermoelectric cryostat lid to remove the heat from the thermoelectric cooler. Before conducting an experiment, the thermoelectric cryostat was pumped to approximately 2×10^{-6} Torr to eliminate condensation on the sample and windows. The seal was maintained by rubber O-rings, which were placed behind each window and under the lid. Power was supplied to the thermoelectric cooler by a Hewlett Packard 6633A DC power supply. Temperature was monitored by a Hewlett Packard 3478A multimeter, which read the temperature-dependent voltage between an Omega Engineering cold junction compensator (icepoint) and the copper plates holding the

Figure 1 – Experimental setup. Reprinted with the permission
of Dr. A. Y. Hamad

sample. This voltage was then converted to temperature based on data supplied by Omega Engineering.

The LIG was formed in these samples by allowing two laser beams (write-beams) to intersect inside the sample with a crossing angle of $2\theta=3.866^0$ (measured in air). All experiments were performed using the output of a cw argon laser operating in the TEM_{00} mode. The Gaussian profile of the beam was confirmed by using a laser beam profiler. The 465.8 nm laser line of the cw argon laser is known to excite the Eu^{3+} ions to the $^5D_2$ level and was used to form the write-beams. By using a beam splitter, the main beam was split into the write beams, and these were redirected by two mirrors to cross at the location of the sample. The optical path lengths of the write-beams were kept equal to within the coherence length of the laser. The write-beams were focused using two lenses, each of which had a 50cm focal length. The diameter of each beam was measured to be 154 μm ± 2 μm using the beam profiler. The total power of the write-beams was in the range of 20-50 mW.

LIG were detected using 632.8nm light from a He-Ne laser, which was counter propagated along one of the write-beams at a slightly different angle. We refer to this as the read-beam. The read-beam was focused so that its diameter at the position of the sample was 180 μm and filled the LIG. A translatable, rotatable mirror was used to direct the read-beam to the LIG so that the Bragg condition was satisfied enabling maximum diffracted power. The power of the read-beam at the sample surface was 3 mW.

The diffracted signal was detected by a Hamamatsu R1547 photomultiplier tube (PMT), which was connected to a PC via an EG&G Ortec ACE-MCS multichannel

scaling card. Stray argon light and sample fluorescence were eliminated from detection by placing an interference filter at 632.8 nm in front of the PMT. To get absolute magnitudes for the power of the diffracted signal, we calculated a calibration factor for the output voltage of the PMT using different neutral density filters and the known 3 mW power of the He-Ne laser. Using this calibration factor, we were able to obtain the diffracted power in absolute units by measuring the PMT output voltage.

The index of refraction of each sample at the read and write wavelengths, n_r and n_w, was measured using the Brewster angle technique [12]. The sample absorption coefficients, α_r and α_w, were measured at each wavelength using a Cary 05 spectrophotometer, which has a photometric accuracy of $\pm\, 0.001$.

Experimental Procedure

The same technique for FWM at room temperature was used to form LIG below room temperature. This technique has been described by Hamad *et al.* [9]. Prior to forming the LIG, the sample was placed in the pumped thermoelectric cryostat described above, and the temperature was lowered by adjusting the voltage applied to the thermoelectric cooler. When the sample arrived at the desired steady-state temperature, we took a 30-second background reading and then began to write the LIG. During the grating formation process, the temperature was held constant to within 1K.

Typical scans below room temperature are shown in Figure 2 for Eu2.5 and Figure 3 for Eu5. The characteristics of grating formation studied in this thesis included:
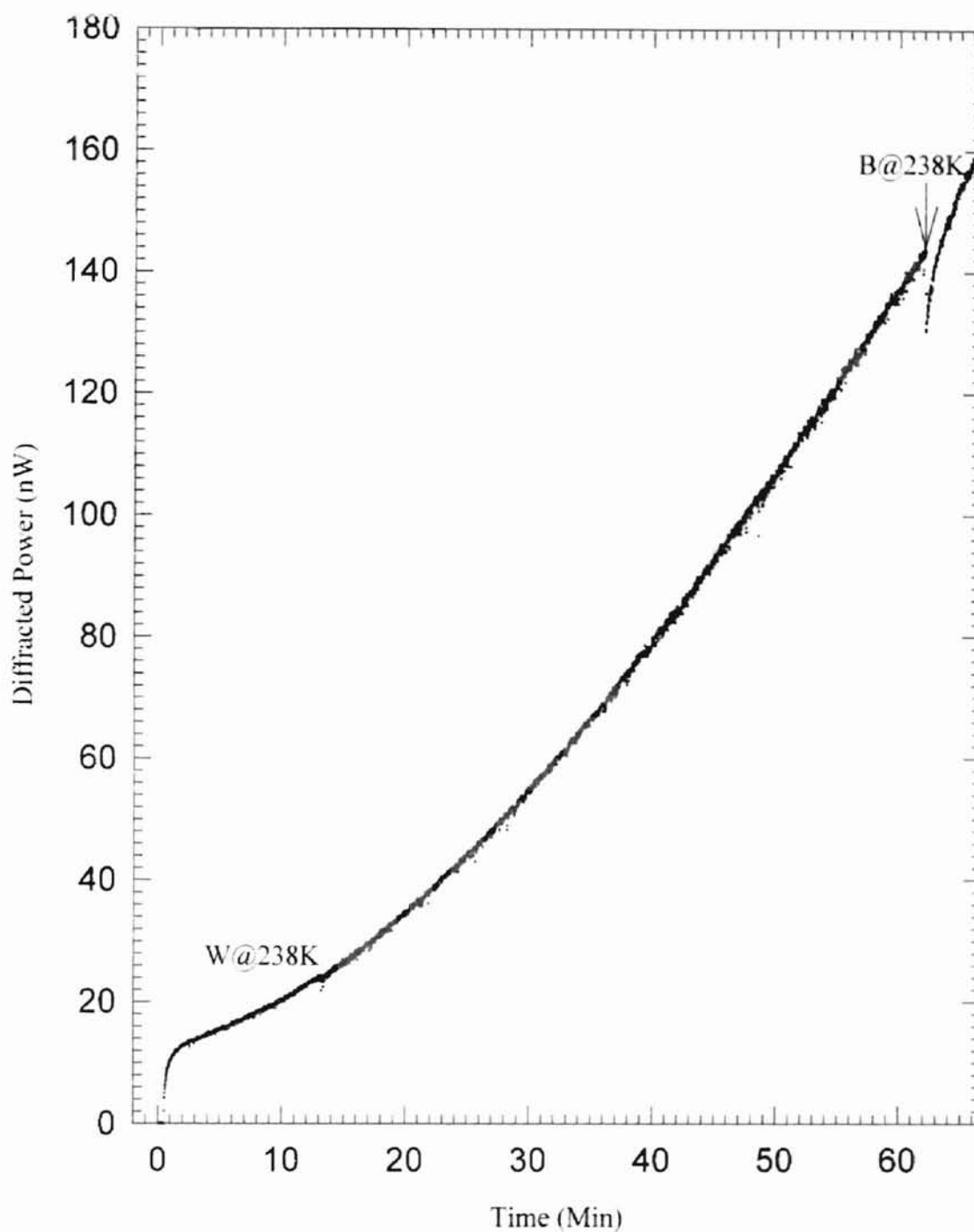
Figure 2 - Diffracted power during grating formation in Eu2.5 at 238K with a write-beam power of 50mW. W - write, B - block.
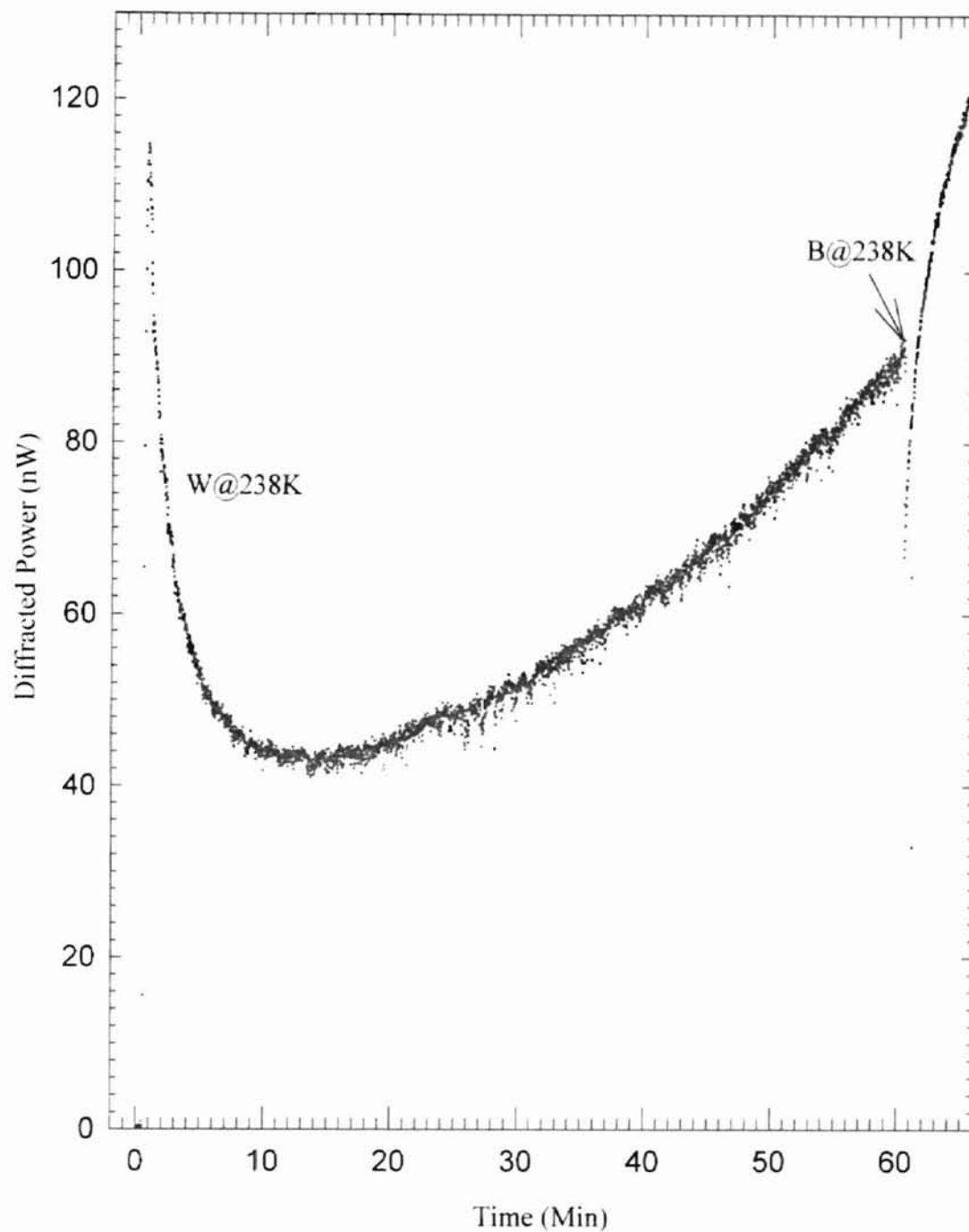
Figure 3 - Diffracted power during grating formation in Eu5 at 238K with a
write-beam power of 50mW.

initial diffracted power maximum, P_i, initial maximum buildup time, t_{bld}, time to minimum, t_{min}, write time maximum, P_{Wmax}, and the behavior after write-beam blockage[1]. The variation of these LIG formation characteristics was studied as several experimental factors were varied. These factors included sample Eu^{3+} concentration, write time, block time, temperature, and write-beam power. All experiments were conducted at each of the three temperatures mentioned above.

Of particular interest in these experiments was the LIG that remained at room temperature after being formed at low temperature. Therefore, after the grating formation process was completed, the samples were returned to room temperature by turning off the voltage supply to the thermoelectric cooler. In the process of warming, the sample expansion caused a corresponding expansion of the LIG. Therefore, it was necessary to re-adjust the angle of the read-beam to satisfy the Bragg condition for maximum diffraction from the expanded grating. The diffracted signal intensity was then measured and compared to the diffracted signal intensity before warming.

All output voltage signals from the PMT were converted to diffracted signal power using the calibration factor described above. In addition, the non-linear change in the index of refraction was calculated using the method described by Hamad *et al.* [13]. This allowed us to compare LIG strength among samples of different thickness' and absorption coefficients. The important parameters involved in this calculation are listed in Table I.

---

[1] Some of these characteristics do not apply to Eu2.5 below room temperature. As can be seen, there is not an initial maximum or a minimum in grating formation. This will be discussed in a later section.

Sample	Length (mm)	Width (mm)	Thickness (mm)	n_w	n_r	α_r (cm^{-1})	α_w (cm^{-1})	R	β
Eu5	12.96	6.28	1.80	1.50	1.49	1.050	0.487	0.039	6.800×10^5
Eu2.5	14.44	6.38	1.88	1.52	1.51	1.419	0.561	0.041	5.725×10^5

Table I - Some of the linear optical parameters for the samples used in the study. R is the reflection coefficient, and β is a parameter as defined by Hamad et al. [13]. R and β were used in the calculation of Δn.

CHAPTER III

EXPERIMENTAL RESULTS

The grating strength can be described by the diffracted signal power or by the non-linear change in index of refraction. At different times in reporting results in this thesis, it was found more appropriate to use one rather than the other to make comparisons and show relationships. However, it should be noted that both the diffracted signal power and the non-linear change in the index of refraction are a measure of the grating strength and are related by the theory of Hamad *et al*.

Unless otherwise stated, all data reported are for a write-beam power of 50 mW. Although other write-beam powers were used, these results will be collected in a separate section.

Eu^{3+} Concentration

As can be seen from Figures 2 and 3, the qualitative behavior of the grating formation process below room temperature in the Eu2.5 and Eu5 samples is very different. When comparing samples, it is important to compare the non-linear change in index of refraction, Δn, instead of diffracted power because the samples have different thickness' and absorption coefficients. Therefore, Figures 4 and 5 show Δn during

Figure 4 - Change in non-linear index of refraction during grating formation in Eu2.5 at 238K with a write-beam power of 50mW.
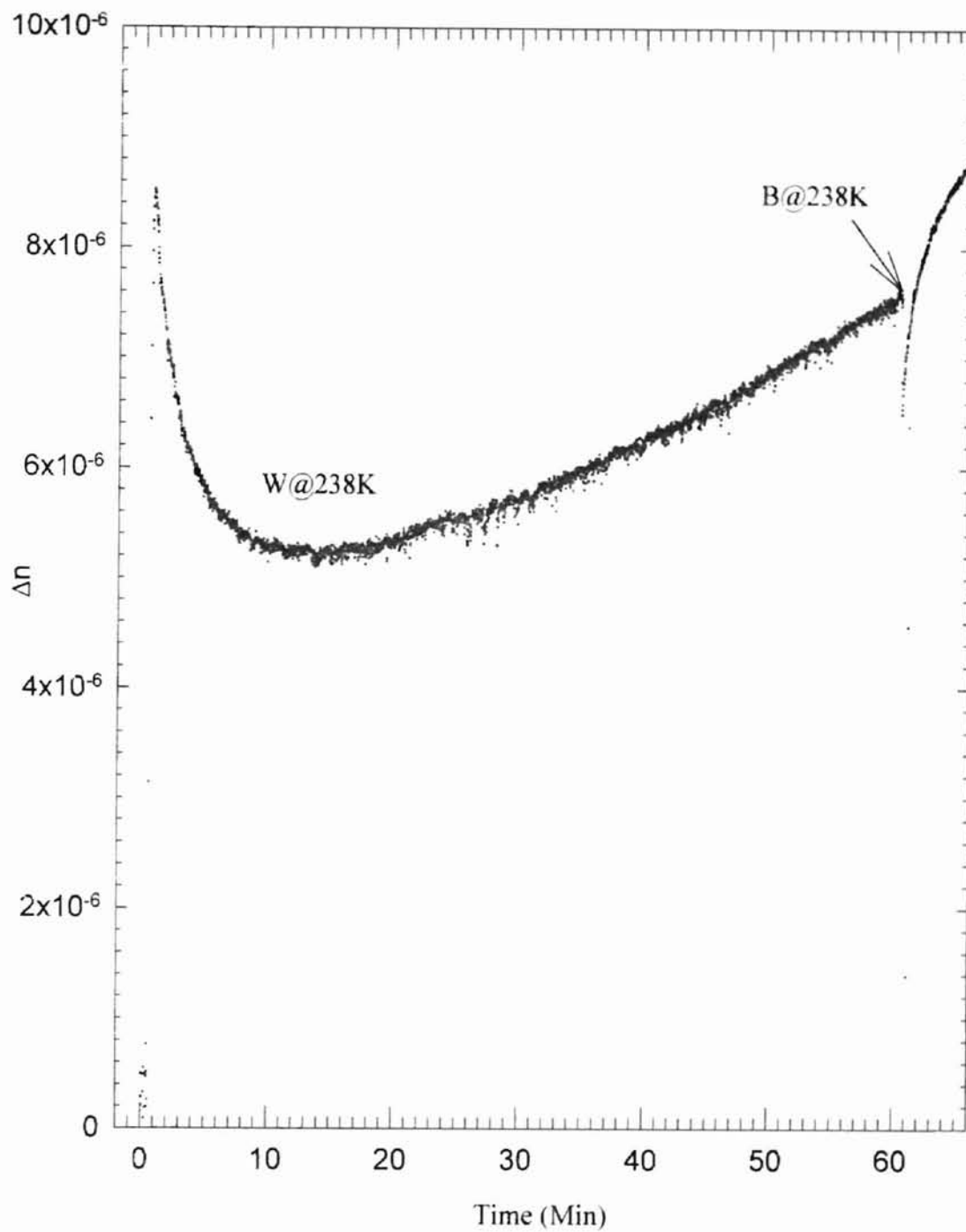
Figure 5 - Change in non-linear index of refraction during grating formation in Eu5 at 238K with a write-beam power of 50mW.

typical grating formation processes at 238K in Eu2.5 and Eu5, respectively. Figures 6 and 7 show the same at 265K. In the Eu5 sample, Δn reaches an initial maximum, falls to a minimum, and then begins a gradual monotonic increase. The Eu2.5 sample does not display a minimum in Δn during the grating formation process. Instead, we see an initial "jump" in Δn, followed by a continuous, monotonic increase.

This difference in the qualitative behavior between samples was only seen below room temperature. At room temperature, both samples displayed the same qualitative behavior: initial maximum falling to a minimum, followed by a gradual monotonic increase. Figures 8 and 9 show the qualitative behavior of the Eu2.5 and Eu5 samples, respectively, at room temperature. Quantitatively, we find large differences between the samples. In Eu5, t_{bld} occurs at 14 seconds and t_{min} occurs at approximately 30 minutes whereas in Eu2.5, t_{bld} occurs at 130 seconds and t_{min} occurs at approximately 9 minutes. Thus we see that the initial maximum occurs much more quickly and the minimum occurs much more slowly in Eu5 at room temperature. It is also seen that Δn at the initial maximum is 2.5 times greater in Eu5 than in Eu2.5. Also, the overall non-linear change in index of refraction after writing for one hour is 1.6 times greater in Eu5.

Below room temperature, we cannot make the same comparisons between the two samples due to the lack of similarity between qualitative features. We can, however, compare the non-linear change in index of refraction at a given write time. Figures 10 and 11 show the grating formation over a 5 hour period at 238K for samples Eu2.5 and Eu5 respectively. As can be seen, during writing the Eu2.5 sample reaches a change in index of refraction of 5.2×10^{-5} compared to a change of 3.3×10^{-5} for the Eu5 sample. Below room temperature, we found the non-linear change in index of refraction to be
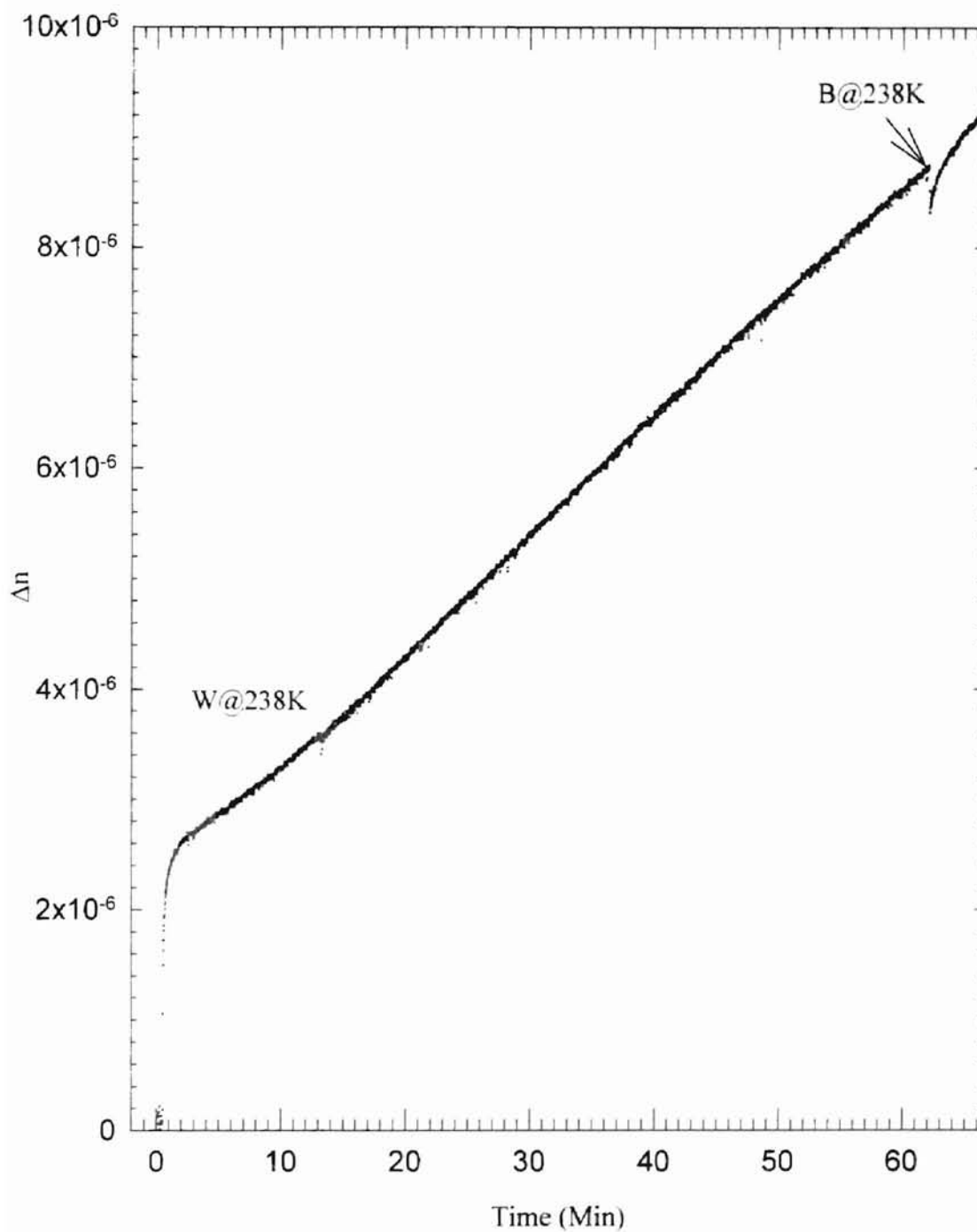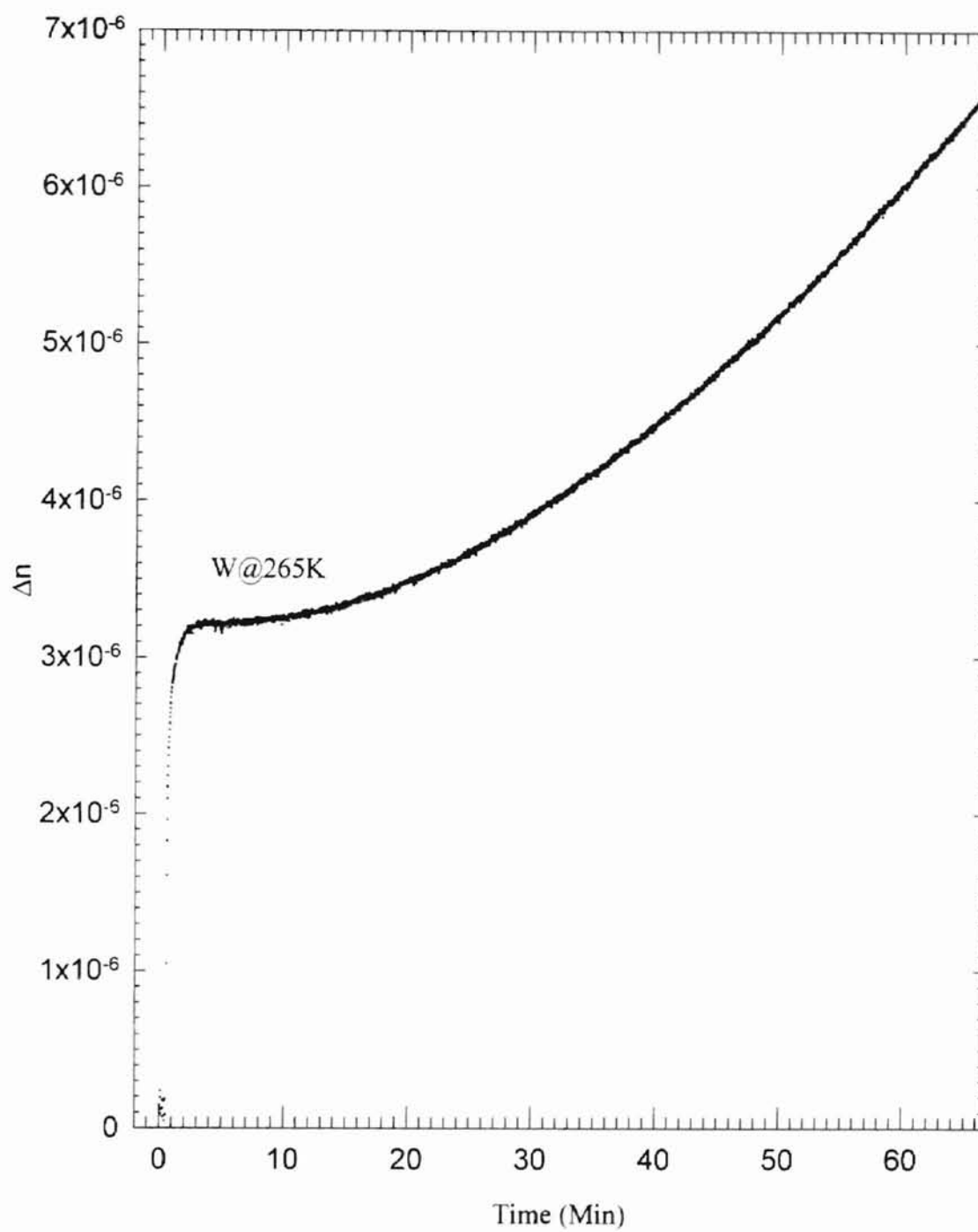
Figure 6 - Change in non-linear index of refraction during grating formation in Eu2.5 at 265K with a write-beam power of 50mW.
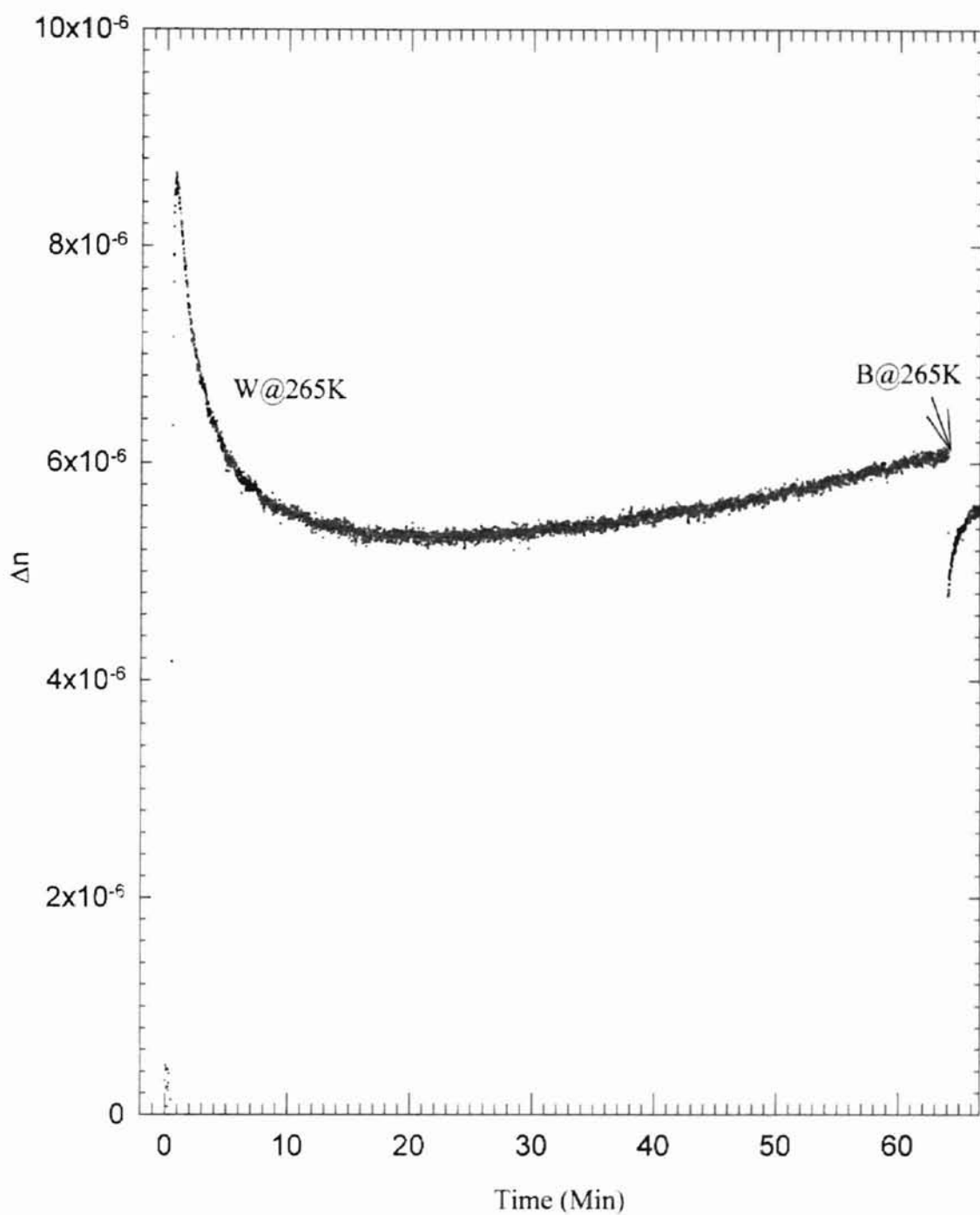
Figure 7 - Change in non-linear index of refraction during grating formation in Eu5 at 265K with a write-beam power of 50mW.
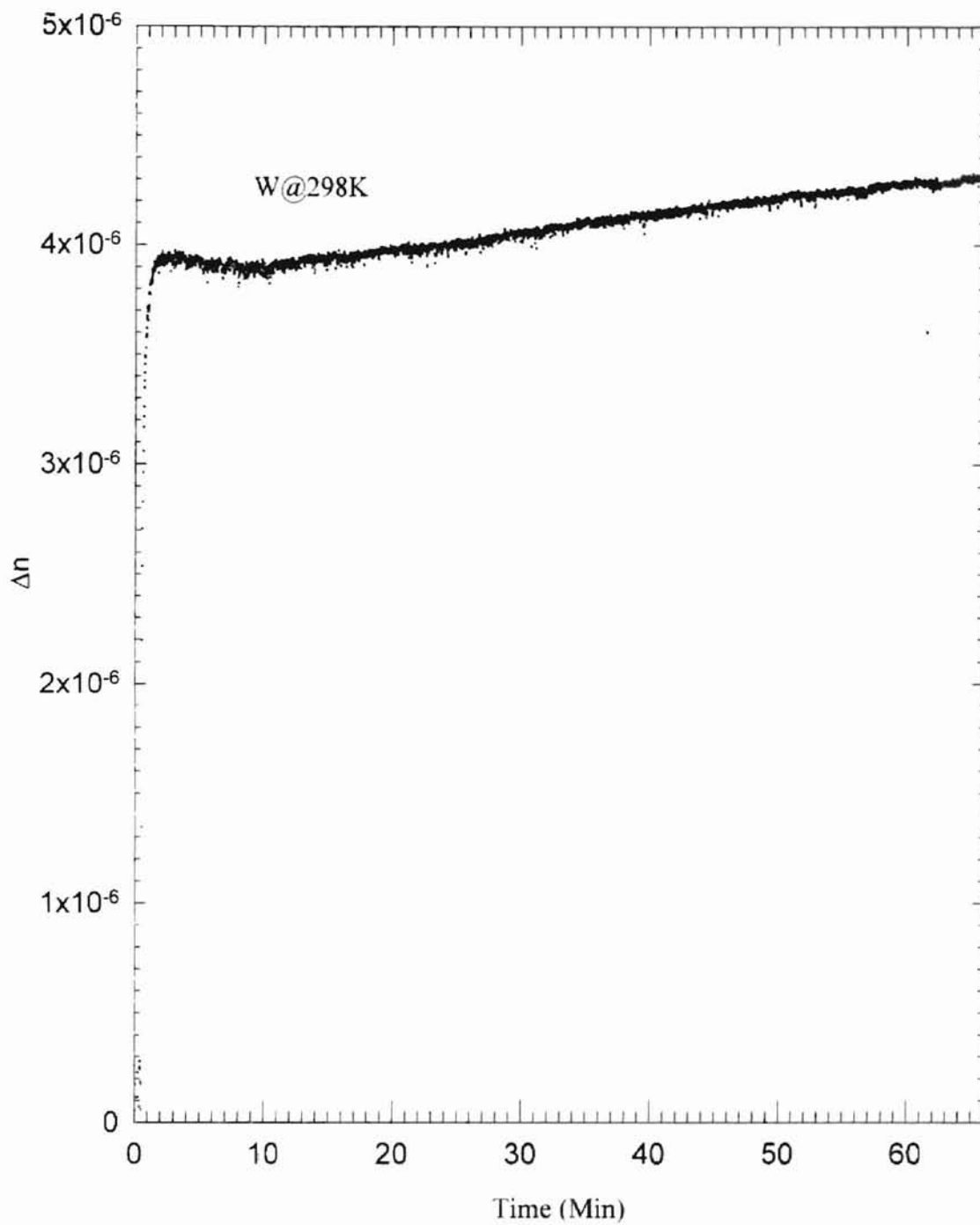
Figure 8 - Change in non-linear index of refraction during grating formation in Eu2.5 at room temperature with a write-beam power of 50mW.
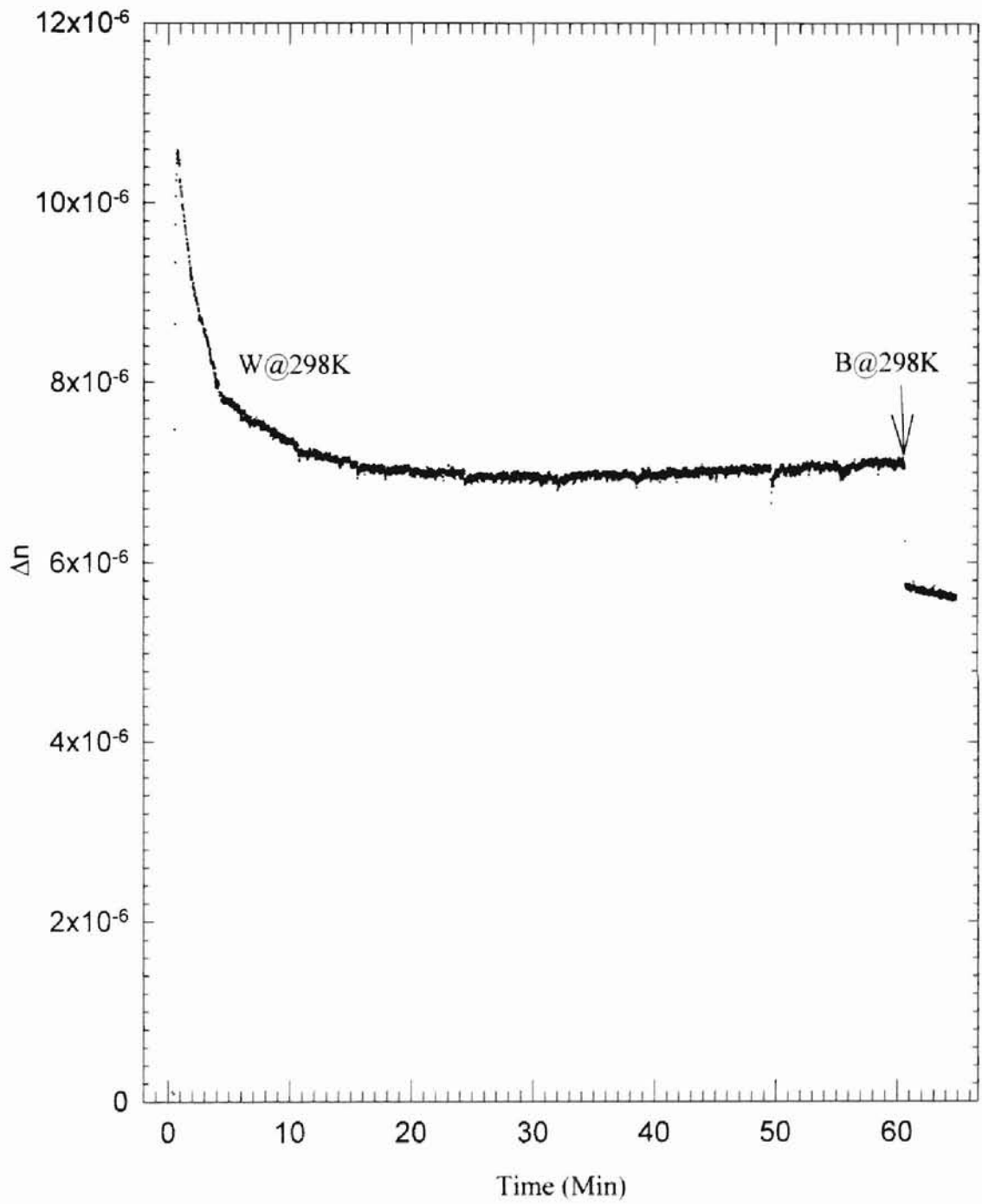
Figure 9 - Change in non-linear index of refraction during grating formation in Eu5 at room temperature with a write-beam power of 50mW.
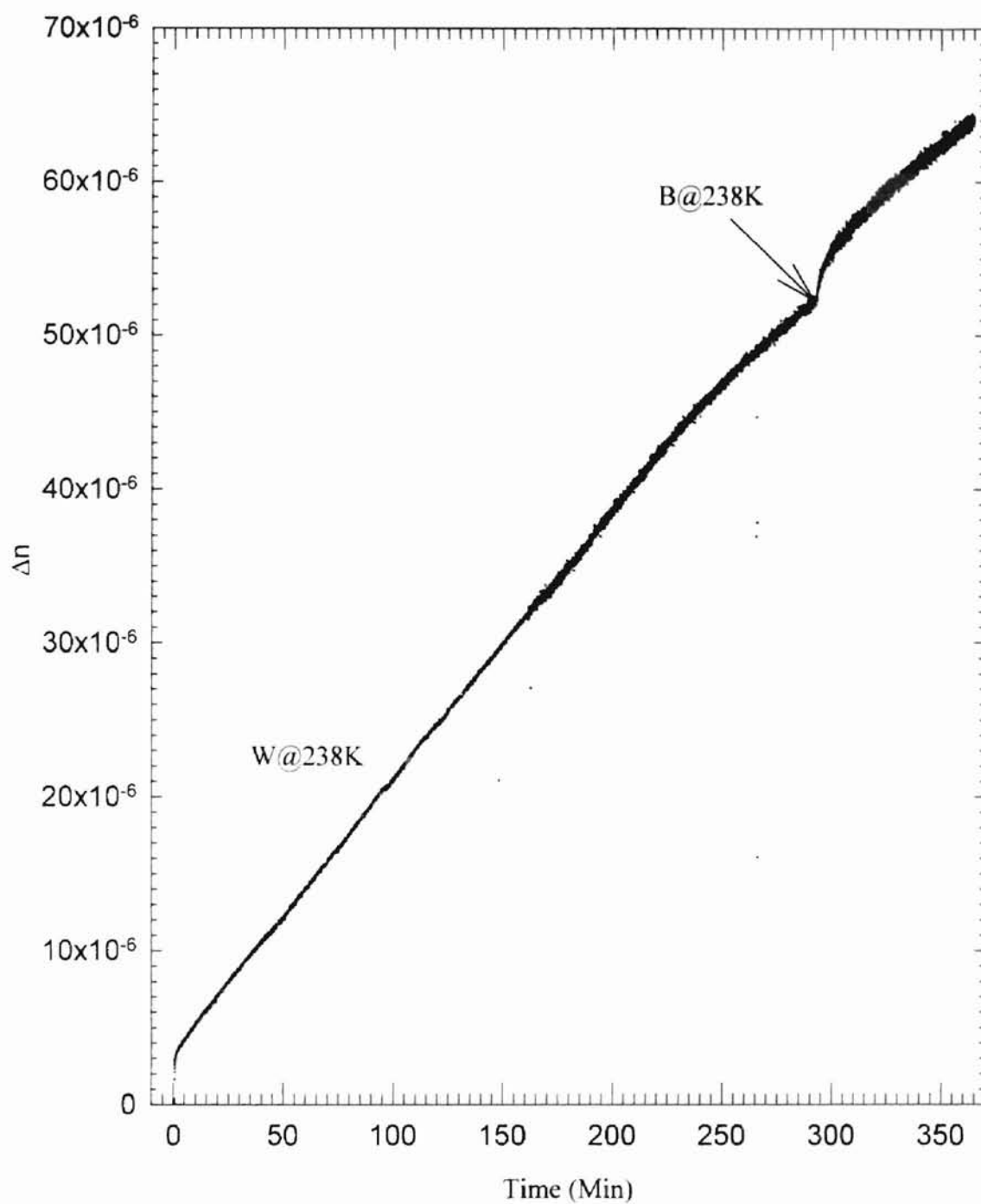
Figure 10 - Change in non-linear index of refraction during grating formation in Eu2.5 for a five hour write period at 238K with a write-beam power of 50mW.
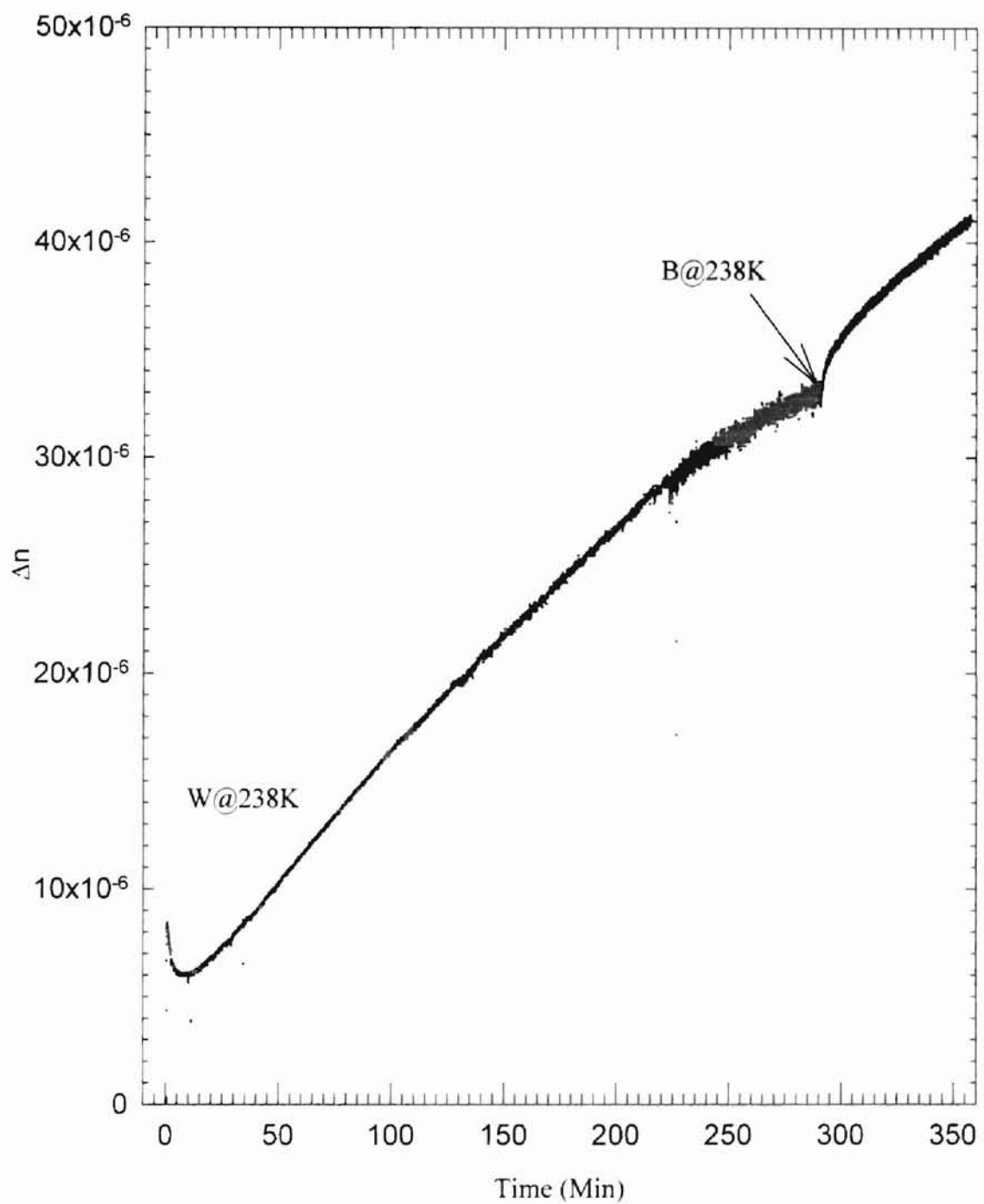
Figure 11 - Change in non-linear index of refraction during grating formation in Eu5 for a five hour write period at 238K with a write-beam power of 50mW.

greatest in Eu2.5 for all write times studied. Table II lists the write times and corresponding change in index of refraction produced in both samples. We also experimented at another temperature below room temperature, 265K, and found the same trend. These results are listed in Table II, along with the results obtained at 238K.

An interesting feature discovered during the experiments conducted below room temperature was the pronounced increase in grating strength that began after the write beams were turned off (block period). In Figures 2 and 3, it can be seen that when the write-beams were blocked, there was a quick drop in diffracted power (due to the transient component of the LIG) followed by a strong increase. The rate of increase during blocking was initially seen to be greater than the rate of increase during writing, however, this rate was seen to slow and eventually level off depending on several factors. The strong increase during blocking was seen only below room temperature and was observed in both samples. We will further discuss this aspect of grating formation in later sections.

Write Time

The dependence of the grating strength on the write time can be quickly deduced from Table II. Longer write times were found to produce stronger gratings. We also found that the write time influences the behavior during blocking. The amount of increase in grating strength during blocking below room temperature was greater for longer write times. In Table III, we have listed the block maximum, P_{Bmax} (maximum diffracted power after blocking), along with P_{Wmax} for each write time. The block time,

Sample	LIG formation Temperature (K)	write time (hr)	Δn_{Wmax} (10^{-6})
Eu5	238	1	9.0
Eu5	238	3	25.0
Eu5	238	5	33.0
Eu2.5	238	1	12.3
Eu2.5	238	3	28.0
Eu2.5	238	5	52.0
Eu5	265	1	5.4
Eu2.5	265	1	7.2

Table II - Typical values of the non-linear change in index
of refraction for various write times

Sample	LIG formation Temperature (K)	write time (hr)	P_{Wmax} (nW)	t_{Block} (hr)	P_{Bmax} (nW)
Eu5	238	1	152	24	4000
Eu5	238	3	530	21	10000
Eu5	238	5	2050	16	18000
Eu2.5	238	1	240	42	11766
Eu2.5	238	3	3500	39	20000
Eu2.5	238	5	9000	34	26500
Eu5	265	1	54	NA	NA
Eu2.5	265	1	82	NA	NA

Table III - Typical values of diffracted power after various write and block times.

t_{block}, has been included as well. For longer write times, it is seen that the corresponding change in grating strength is proportionally greater even though the block times were not as long.

Block Time

As was stated above, an interesting discovery was the increase in grating strength that occurred during blocking. A strong increase in diffracted power was seen in both samples during blocking at 238K and at 265K. However, at room temperature in Eu5 the grating strength was seen to decay during blocking, as seen in Figure 9. At room temperature in Eu2.5, the grating strength was seen to decay during blocking if the grating at the time of blocking was weak. However, if a strong grating was present at the time of blocking, an increase in the grating strength was seen.

We found that after writing a grating below room temperature, the grating strength would continue to increase during blocking for up to 42 hours in some cases. The diffracted power was observed to grow up to 26 μW, and multiple orders of diffraction were clearly visible. The growth in grating strength during blocking at room temperature in Eu2.5 was found to be much smaller than the growth below room temperature and did not continue as long. The diffracted powers reported were contained in the first-order, which was the only order measured. Figure 12 shows a digital photograph of multiple orders of diffraction seen at room temperature. The grating was formed in Eu2.5 at 238K with a write-beam power of 50 mW, a write time of 5 hours.

Figure 12 - Digital Photograph of multiple orders of diffraction obtained from Eu2.5 for a grating formed at 238K with a write-beam power of 50mW, a write-time of 5 hours, and a block time of 1 hour.

and a block time of 1 hour. Table III contains results of the grating strength obtained from different write and block times.

Although long block times below room temperature were seen to create strong gratings in both samples, it was found that the longer the grating was allowed to increase during blocking, the less grating was left when the sample was returned to room temperature. We found anywhere from <1% to 95% of the grating remaining at room temperature depending on the amount of block time. For a given sample, a shorter block time was always seen to give a larger percent of grating remaining at room temperature. Table IV shows results of various write and block times below room temperature and the percent of grating remaining when the sample was returned to room temperature.

Temperature

Figures 13 and 15 show the grating formation during a one-hour write period in Eu2.5 and Eu5, respectively, for all three temperatures studied. Figures 14 and 16 show the first two minutes of Figures 13 and 15 respectively. It can be seen from Figures 13 and 15 that stronger gratings may be formed at lower temperatures.

If we look qualitatively at Figure 13 for Eu2.5, we find that the grating formation behavior changes as the LIG formation temperature is brought below room temperature. It can be seen that there is no longer a minimum[2] in the diffracted power during grating formation below room temperature. Instead, while writing, we see a continual monotonic

---

[2] It is difficult to resolve the minimum at room temperature on this scale, but it is obvious in Figure 8, which is the same room temperature data as depicted in Figure 13.

	LIG formation			% remaining	Diffracted	Δn
Sample	Temperature (K)	Write time (hr)	t_{Block} (hr)	at room temp.	power (nW)	(10^{-6})
Eu5	238	1	0.08	95	145	8.8
Eu5	238	1	24	11	440	15.3
Eu5	238	5	1.2	93	3070	40.4
Eu5	238	5	16	68	12250	80.6
Eu2.5	238	5	1	75	18000	106.8
Eu2.5	238	5	34	<1	100	8.0

Table IV - Percent of grating remaining at room temperature for various below-room temperature write and block times. Included are the actual diffracted power and non-linear change in index of refraction remaining at room temperature.

Figure 13 - Diffracted power during grating formation in Eu2.5 at 298K, 265K, and 238K with a write-beam power of 50mW.

Figure 14 - Diffracted power during first two minutes of grating formation in Eu2.5 at 298K, 265K, and 238K with a write-beam power of 50mW.
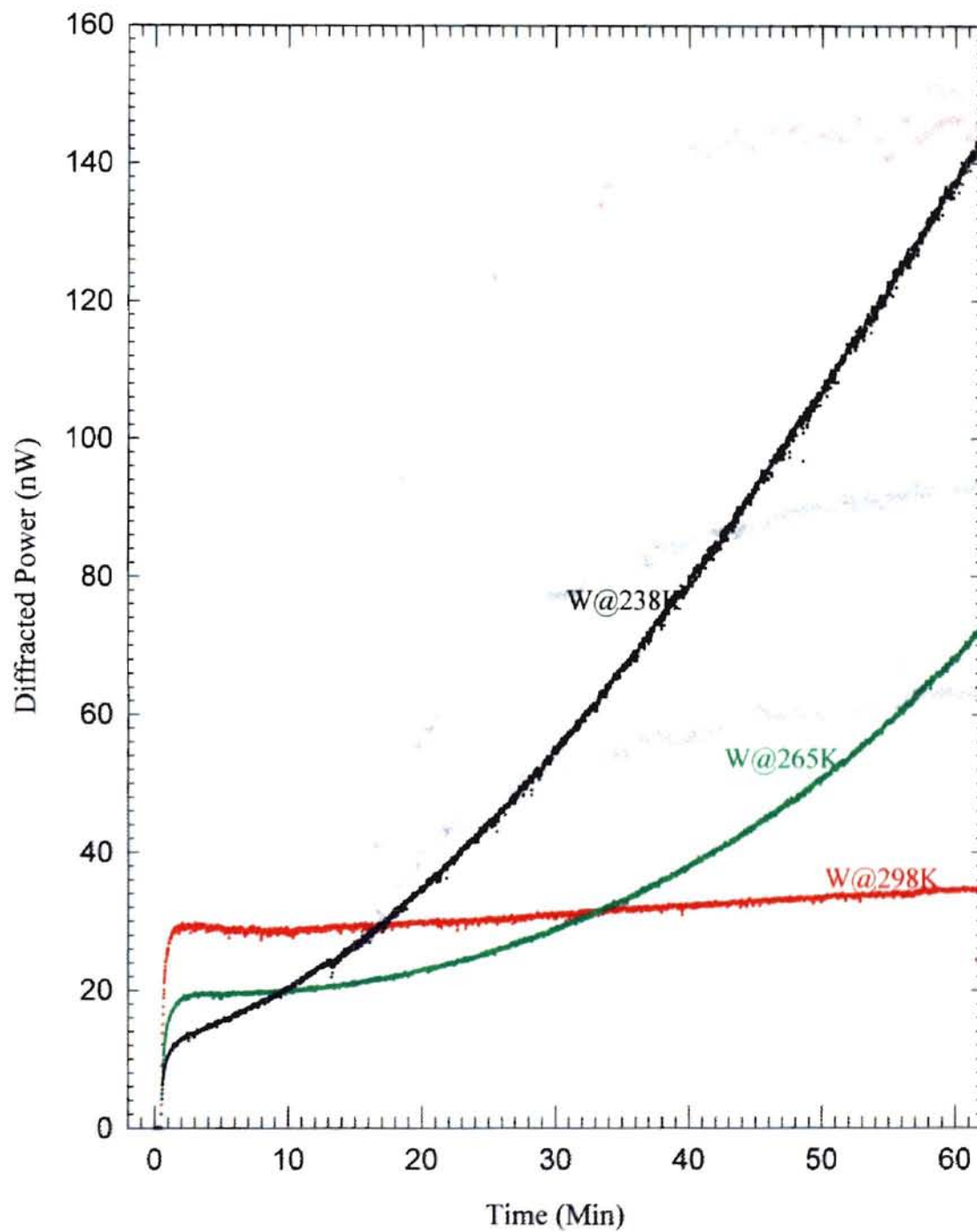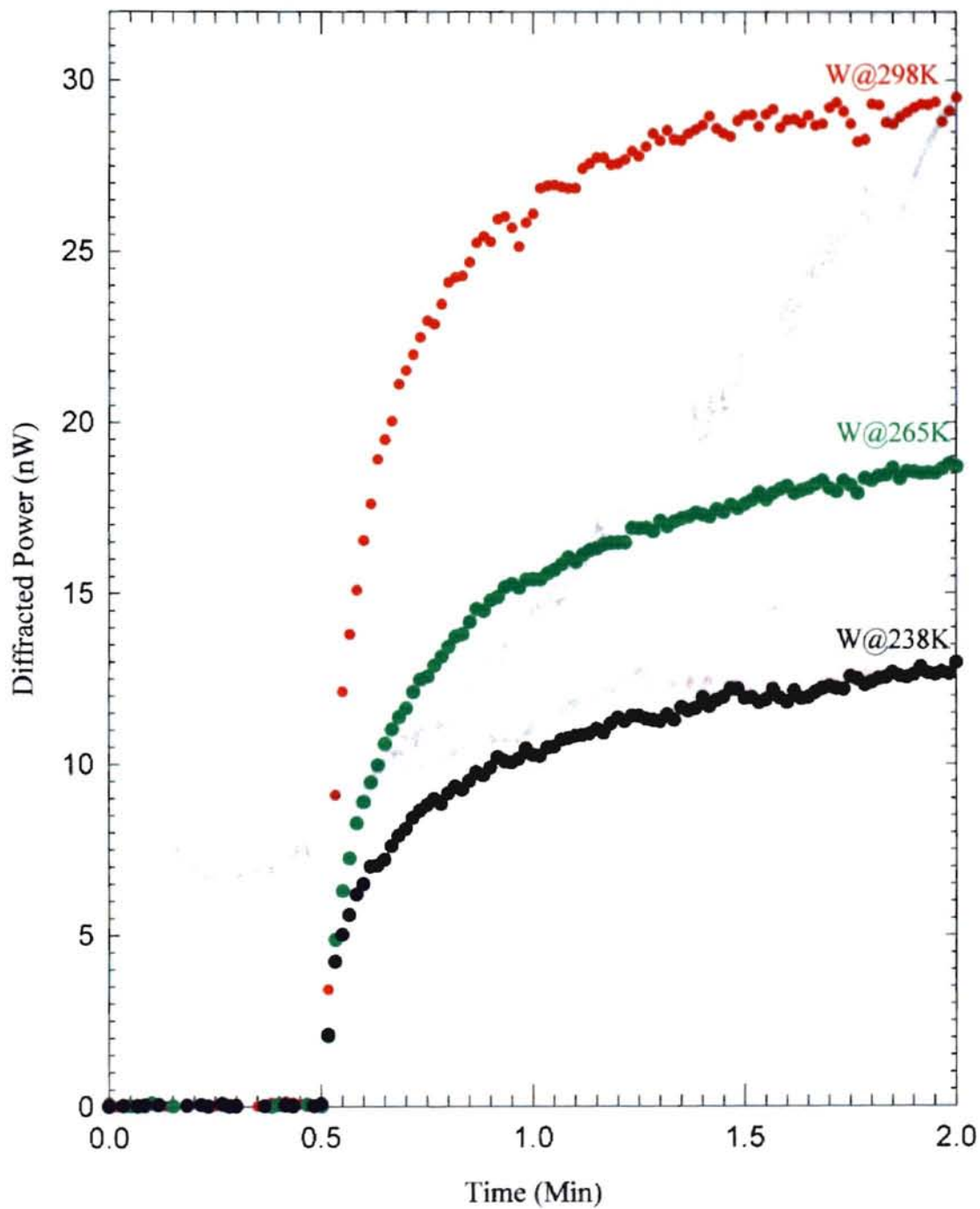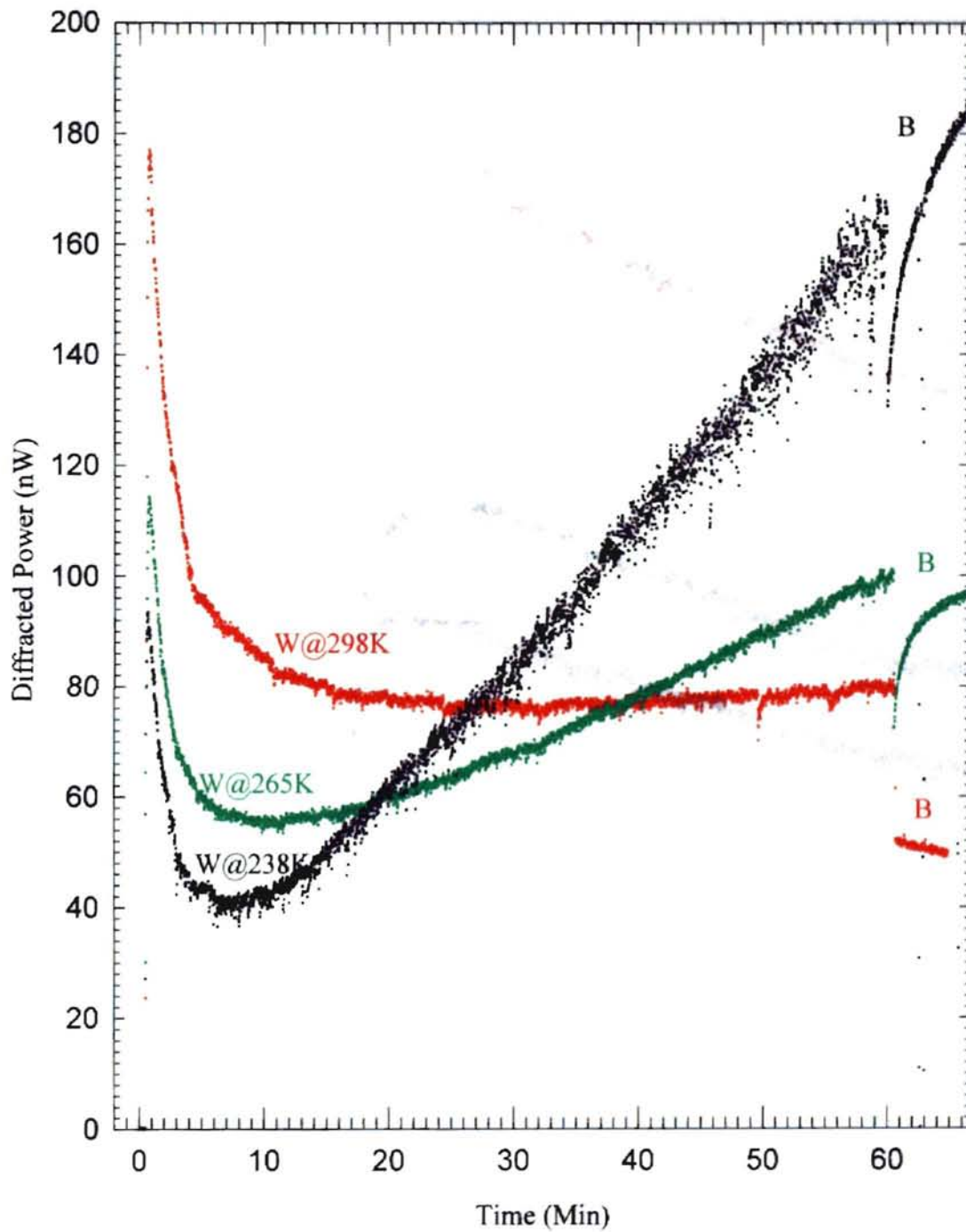
Figure 15 - Diffracted power during grating formation in Eu5 at 298K, 265K, and 238K with a write-beam power of 50mW.
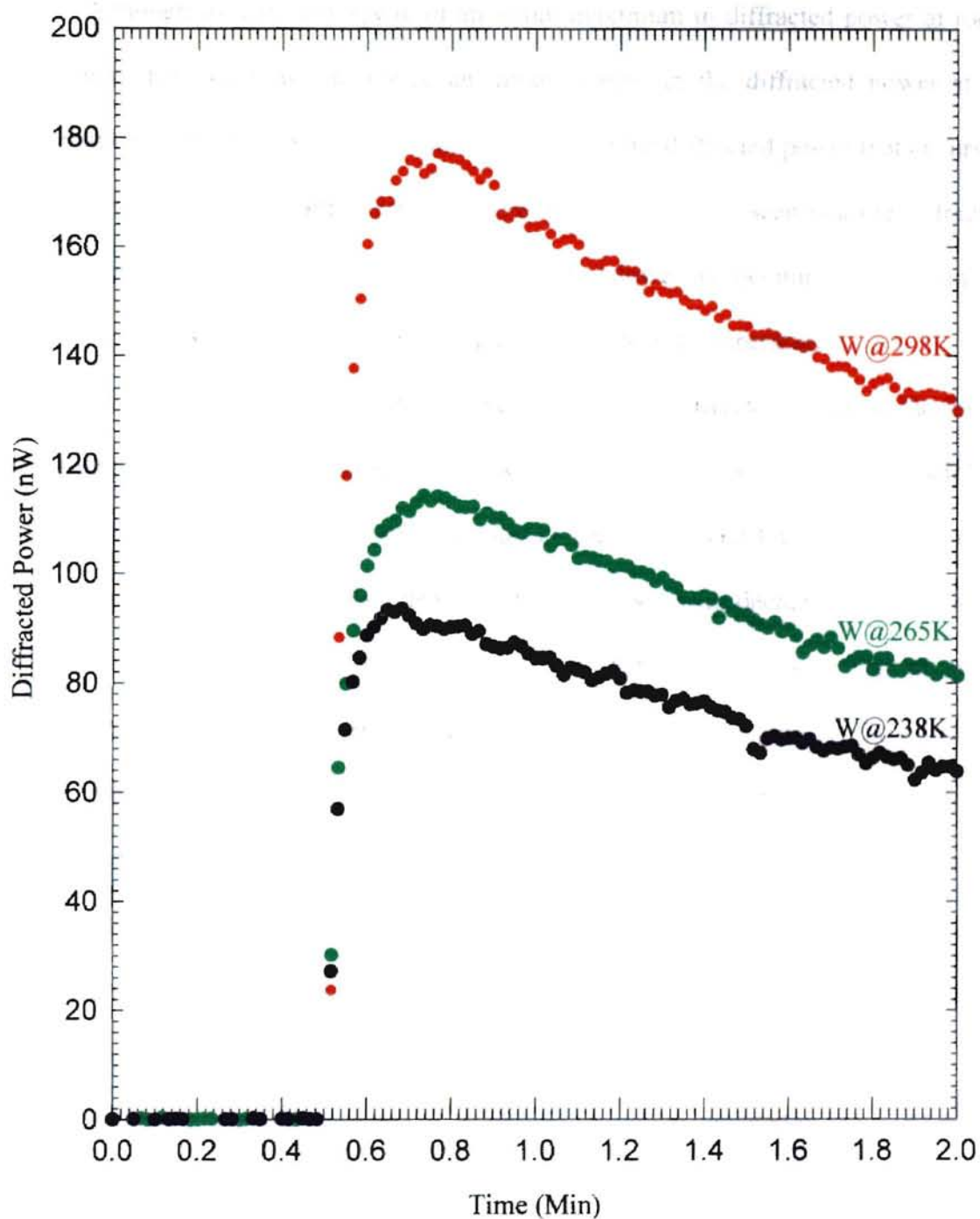
Figure 16 - Diffracted power during first two minute of grating formation in Eu5 at 298K, 265K, and 238K with a write-beam power of 50mW.

increase in diffracted power. Also, it is easily seen that the rate of increase in the diffracted power during writing is much greater at lower temperature.

Although we can only speak of an initial maximum in diffracted power at room temperature for Eu2.5, we do notice an initial "jump" in the diffracted power at all temperatures. The initial jump is the sharp increase in the diffracted power that occurs in the first few seconds of grating formation. From Figure 14, it is seen that the diffracted power after the initial jump begins to limit sooner at lower temperatures. Furthermore, the diffracted power around the initial jump is lower at lower temperatures.

From Figures 15 and 16 for Eu5, we find that the diffracted power at the initial maximum decreases as the temperature is lowered. We also see that t_{bld} decreases slightly as the temperature is lowered. This is similar to the results seen for the initial jump in Eu2.5. From Figure 15, it is also clear that t_{min} decreases with decreasing temperature, and the rate of increase in diffracted power after the minimum is greater at lower temperature. This is again similar to the results seen in Eu2.5. In Figure 17, the diffracted powers from Figure 15 have been normalized so that each initial maximum is unity. It can be seen that the rate of decay after the initial maximum is greater at lower temperature. Also shown in Figure 17 is the similarity of the ratio P_i/P_{min} at each temperature, where P_{min} is the diffracted power at the minimum. Thus, as P_i decreases, P_{min} decreases so as to keep the ratio constant. This can be seen in Figure 15.

Another interesting characteristic of grating formation depicted in Figure 15 is the temperature dependent behavior during write-beam blocking. It can be seen that at room temperature, the grating strength decreases during blocking, whereas below room temperature the grating strength increases during blocking. In addition, below room
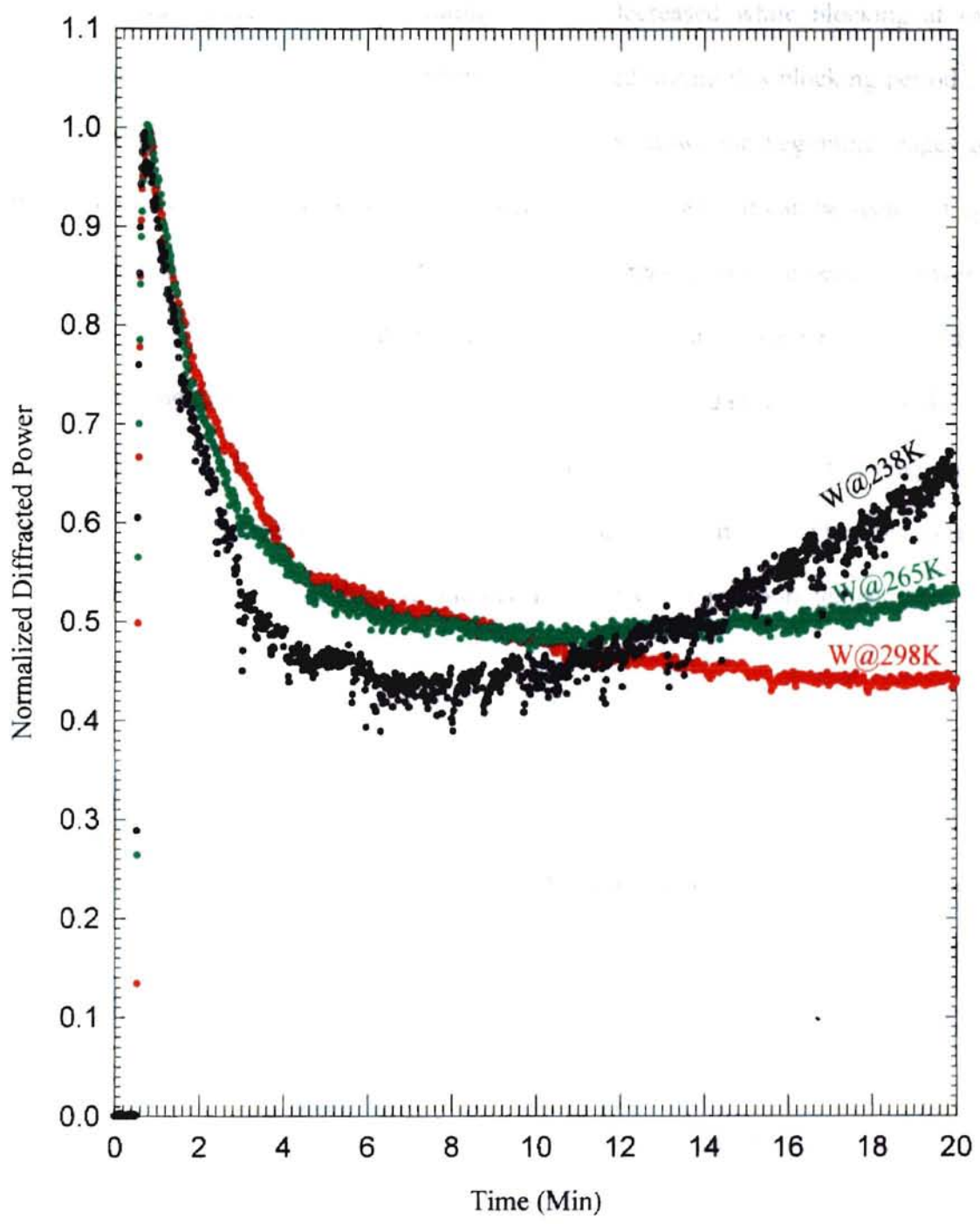
Figure 17 - Normalized diffracted power for initial stages of grating formation in
Eu5 at 298K, 265K, and 238K with a write-beam power of 50mW.

temperature, the rate of increase in grating strength during blocking was greater for lower temperature. This same behavior was noticed in Eu2.5 as well.

As was stated above, the grating strength decreased while blocking at room temperature. However, if the temperature was lowered during this blocking period[3], the grating strength would begin to increase. Figure 18 shows the beginning stages of a grating formed at room temperature, and then cooled to 238K. It can be seen that upon blocking at room temperature, the diffracted power decreased until we began to lower the temperature. After some fluctuation, during which the temperature was approaching a steady state, the diffracted power and thus grating strength began to increase, and did so for over 15 hours. Figure 19 shows the full scan. After this period of grating growth during blockage, we returned the sample to room temperature and found that we were left with a 200% stronger grating than we initially had after writing at room temperature.

Write-Beam Power

To study the effect of write-beam power on LIG formation, we used sample Eu5 and used write-beam powers of 20mW, 30mW, and 50mW. The write-beam power experiments were conducted at 265K and 238K, but not at room temperature. Room temperature write-beam power dependence results have been documented by several other authors [4,9,11].

Figures 20 and 21 show the power dependence at 265K and 238K, respectively. In the first few minutes of grating formation, we see the same qualitative behavior at both temperatures: P_i is greater for higher power, t_{bld} is smaller for higher power, and t_{min} is

---

[3] Unless otherwise stated, all LIG formation was carried out at a single temperature to within 1K.
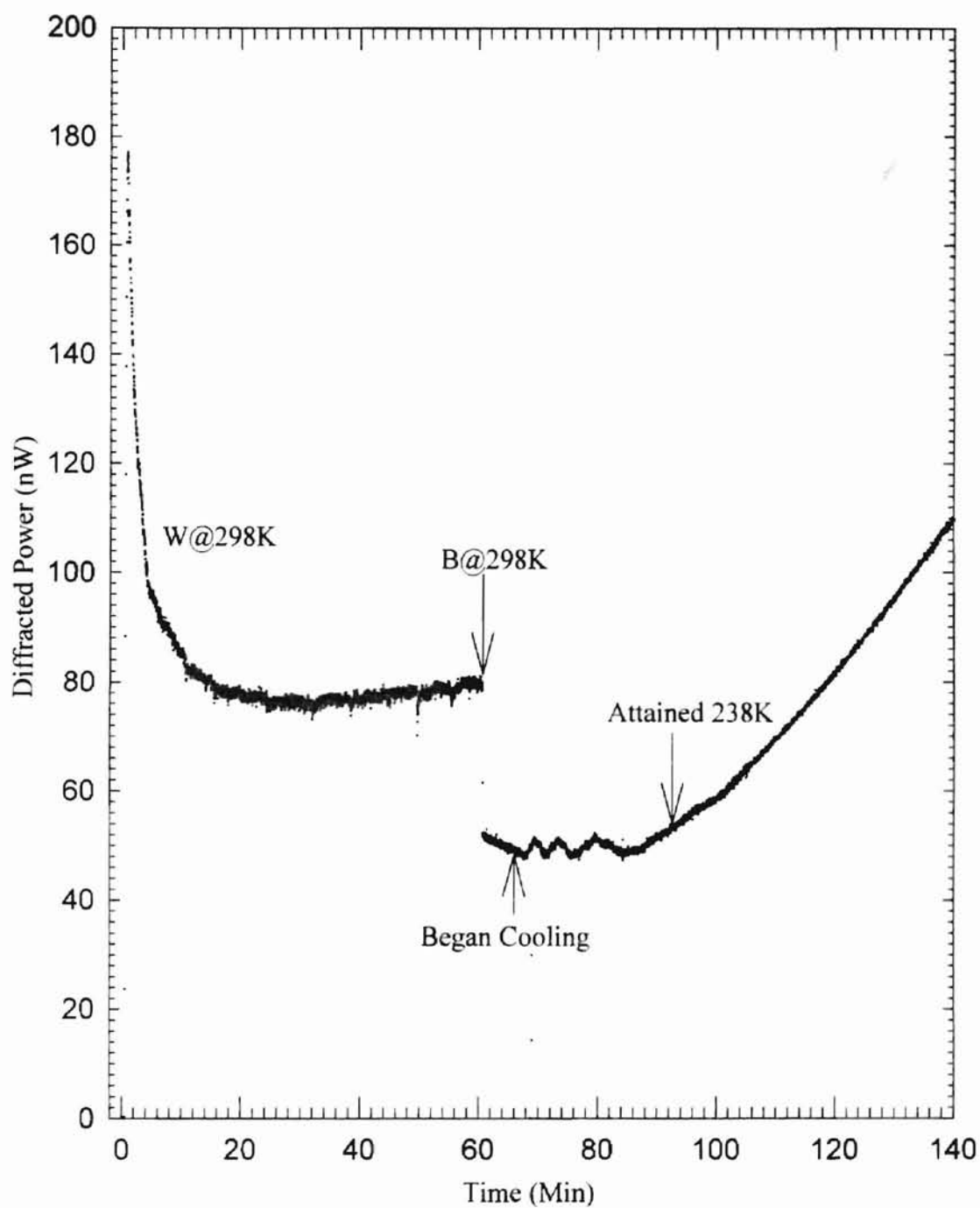
Figure 18 - Diffracted power during initial stages of grating formation in Eu5 at room
temp. with a write-beam power of 50mW. Also shown is the increase in
grating strength while cooling during blocking.
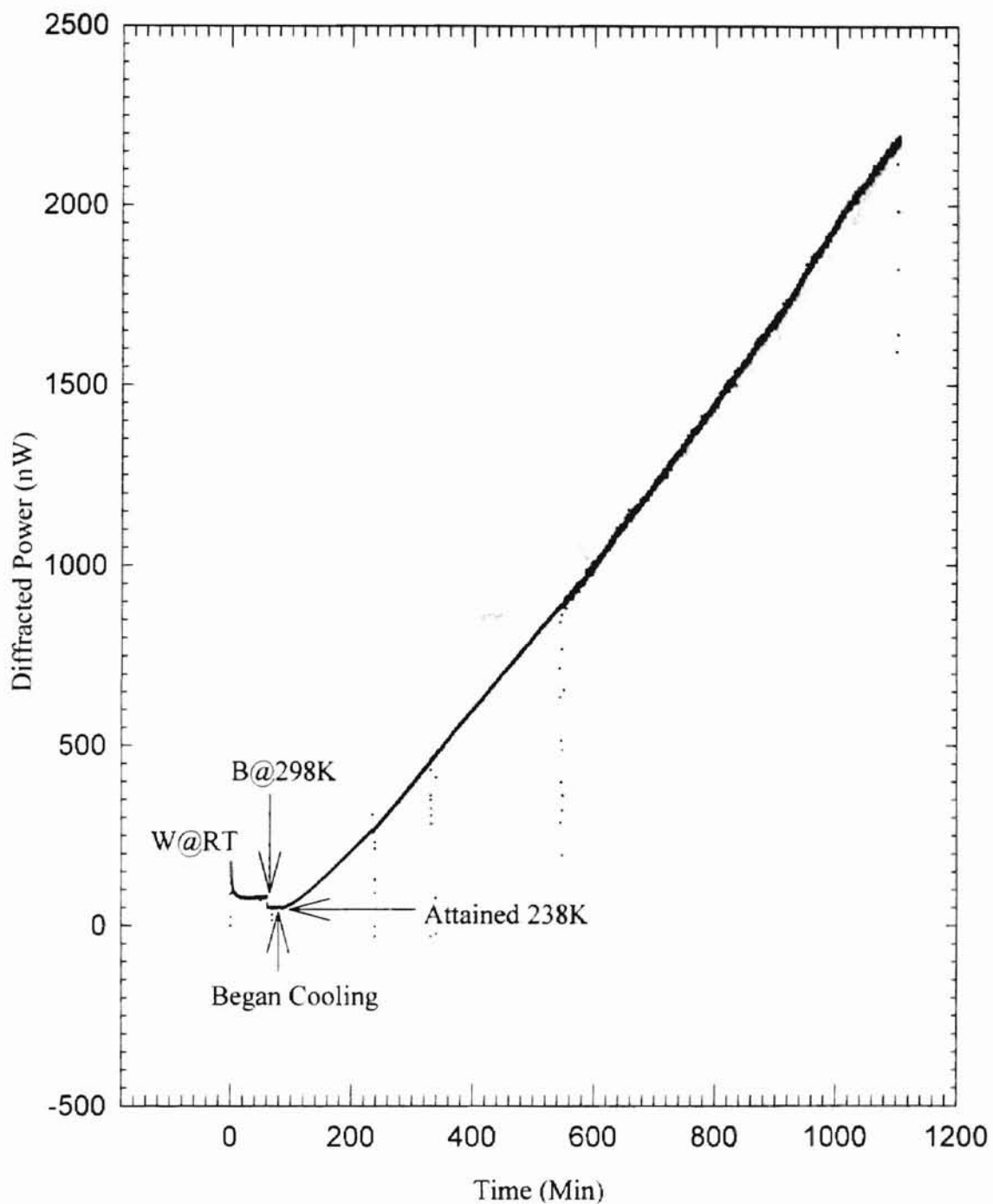
Figure 19 - Diffracted power during grating formation in Eu5 at room temperature with a write-beam power of 50mW. During blocking, the temperature was lowered to 238K.
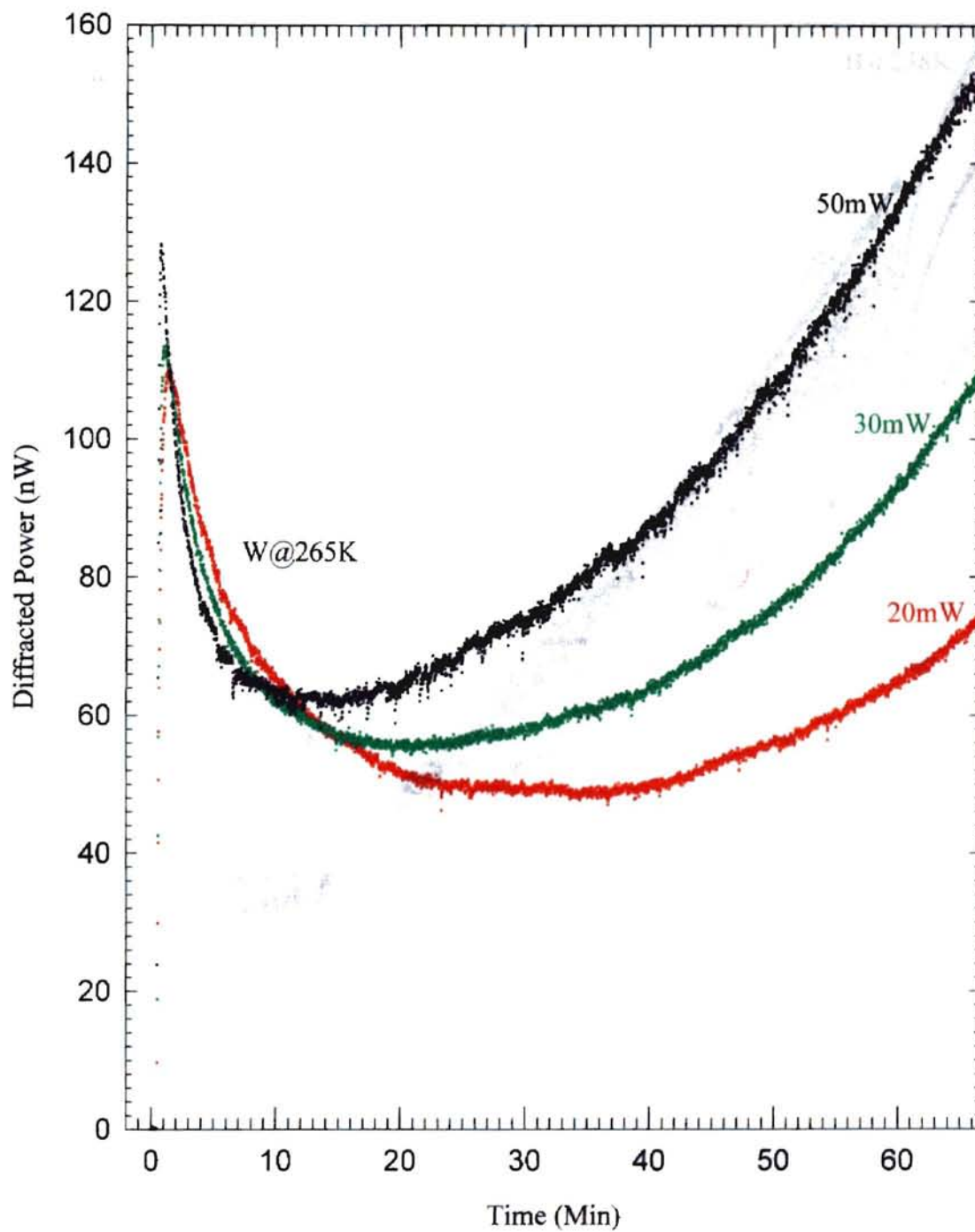
Figure 20 - Diffracted power during grating formation in Eu5 at 265K for write-beam powers of 20mW, 30mW, and 50mW.
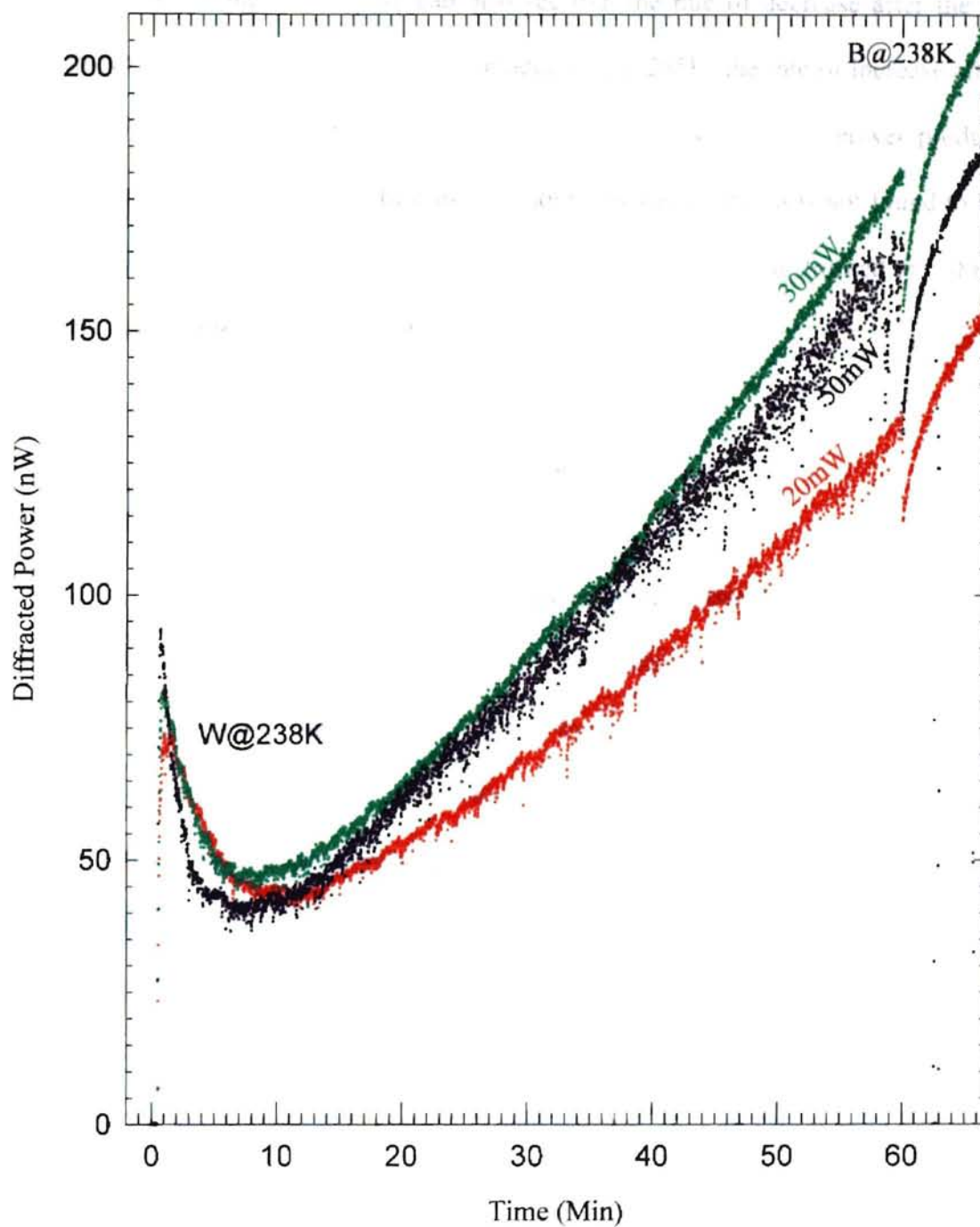
Figure 21 - Diffracted power during grating formation in Eu5 at 238K for write-beam powers of 20mW, 30mW, and 50mW.

smaller for higher power. Table V lists the values for each of these power dependent variables, along with the temperature at which the particular LIG was formed.

At both temperatures, we can also see that the rate of decrease after the initial maximum is greater for higher power. In addition, at 265K, the rate of increase after the minimum was greater for higher power. Thus a higher write-beam power produced a much stronger grating after writing for one hour. However, this was not found to be the case at 238K. As can be seen in Figure 21, the strongest grating formed at 238K was produced at a write-beam power of 30mW.

Summary

The results of the FWM experiments reported above have shown that much stronger gratings may be formed below room temperature with the capability of retaining 95% of the grating after returning the sample to room temperature. We found that the strongest gratings were produced below room temperature when we wrote for five hours[4], and we found that a larger portion of this grating remained at room temperature if we blocked for less time. We also found that stronger gratings could be formed in Eu2.5 than in Eu5.

Table VI shows the maximum grating strength at room temperature for LIG formed below and at room temperature in both samples. For an LIG formed below room temperature, the room temperature maximum diffracted power reported was the diffracted power remaining after the sample was returned to room temperature. For an

---

[4] As compared to one hour or three hours, which were the write times studied in these experiments.

Sample	LIG formation Temperature (K)	Write-beam Power (mW)	P_i (nW)	t_{bld} (s)	t_{min} (s)
Eu5	265	20	111	46	1800
Eu5	265	30	114	32	1200
Eu5	265	50	129	15	840
Eu5	238	20	74	41	690
Eu5	238	30	82	28	510
Eu5	238	50	93	13	491

Table V - Some power dependent characteristics of grating formation

	LIG formation			Diffracted pwr. remaining	
Sample	temp. (K)	write time (hr)	t_{Block} (hr)	at room temp. (nW)	Δn (10^{-6})
Eu2.5	238	5	1	18000	106.8
Eu2.5	238	5	34	100	8.0
Eu5	238	5	1.2	3070	40.4
Eu5	238	5	16	12250	80.6
Eu2.5	298	5	NA	660	20.4
Eu5	298	5	NA	178	9.7

Table VI - Diffracted power and corresponding non-linear change in the index
of refraction remaining at room temperature for LIG formed at
and below room temperature.

LIG formed at room temperature, the maximum diffracted power obtained during grating formation was reported.

From Table VI, we see that there are particular requirements for obtaining strong gratings below room temperature. In a previous section we stated that, in both samples, shorter block times yielded a larger percent of the grating strength remaining when the sample was returned to room temperature. We also stated that, in both samples, the grating strength increased dramatically while blocking below room temperature. Thus there must be a block time for which the grating remaining at room temperature is maximized with respect to both of these variables.

We found that the block time that gives the strongest grating remaining at room temperature was sample dependent. For Eu2.5, we found that writing for five hours, and blocking for around one hour gave the strongest grating remaining at room temperature. For Eu5, we found that writing for five hours, and blocking for around 16 hours gave the strongest grating remaining at room temperature. We observed that forming the gratings below room temperature, according to the procedures stated above, produced gratings that were much stronger than gratings produced at room temperature.

CHAPTER IV

DISCUSSION

Room Temperature Results

The results reported in this thesis for LIG formation at room temperature do not seem to be in agreement with results that have been reported by previous authors [1-9]. As described above, during grating formation at room temperature, we noticed an initial maximum in diffracted power, followed by a minimum, and then a gradual monotonic increase. Previous experiments conducted by Hamad *et al.* [9] do not show a minimum or subsequent increase in diffracted power during grating formation. In the experiments conducted by Hamad. the diffracted power was seen to reach a maximum, followed by a decay that continued for the remainder of the one hour write period. In our room temperature experiments, we noticed the minimum in grating strength within 30 minutes.

A possible explanation [14] for the differences in the results lies in the way that the samples were held during experimentation. In Hamad's experiments, the sample was fixed to an adjustable platform with an adhesive. In our experiments, the sample was placed within the dewar between two copper plates. The copper plates would have efficiently conducted away any heat produced by the laser write-beams, whereas no heat conduction would have occurred in Hamad's experiment. Thus, putting the sample between the copper plates in the dewar would have effectively cooled it, and we would

expect to see results consistent with LIG formation below room temperature. In our experiments, we found that as the temperature was lowered, t_{min} decreased. Thus, the minimum observed at room temperature would not be unexpected if a cooling effect were occurring.

Permanent Grating Formation

The qualitative behavior of grating formation described in this thesis is, to our knowledge, the first time this behavior has been seen. Previous experiments [1-9] have described a maximum in grating strength, followed by a decay for continued writing. However, there are no reports of an increase in grating strength after a minimum. This leads us to propose a modified description of the mechanism responsible for permanent grating formation.

Our results are indicative of competing processes during grating formation. The competition of these processes results in the minimum in grating strength during grating formation. In addition, the initial maximum and the increase in the grating strength after the minimum are understood if one process is initially dominant, and the other process dominant after longer write times.

The model of Dixon et al. [11] attributes grating formation to the long-range migration of small modifiers from the illuminated regions toward the dark regions of the interference pattern formed by the write-beams. Recent self-lensing experiments conducted by Hamad et al. [15] have suggested that this creates two regions in the

material with positive Δn. Based on the time dependence of lens formation and x-scan[5] data, a positive Δn is proposed to occur in the center of the illuminated region, where the modifiers diffuse from due to a change in the polarizability. In addition, a positive change in Δn is proposed to occur around the edge of the illuminated region due to an increased concentration of modifiers that migrate there. If, in FWM, each of the illuminated regions in the sample behaves similar to the illuminated region in a self-lensing experiment, then we are effectively creating two gratings in the sample. One grating corresponds to the regions where the modifiers are migrating from, and the other corresponds to the regions where these modifiers are building up. We suggest that the interference of these two gratings is responsible for the behavior in grating formation observed in these experiments.

Figure 22 (a) shows the interference pattern formed at the center of crossing of two gaussian write-beams. Although this pattern changes throughout the region of crossing, the width of each peak remains the same, with only the relative intensities of each peak changing. Thus, we may use the interference pattern at the center of write-beam crossing to discuss the qualitative features of LIG formation. As can be seen from Figure 22 (a), the interference of two gaussian beams in a FWM experiment produces many overlapping illuminated regions with gaussian profiles. In this case, the profiles are two-dimensional instead of three-dimensional. If each of the illuminated regions of the interference pattern behaves similarly to the single gaussian beam illuminated region as suggested, then a positive Δn will be produced at the center and at the edges of each illuminated region in the interference pattern. Since the edges of the illuminated regions

---

[5] Intensity is monitored as the lens is probed in a direction perpendicular to the write-beam.

overlap in the interference pattern, there will be some overlap of the modifiers that migrate to the edges of each illuminated region. Over time, this will create a large positive Δn in the regions between the illuminated regions (dark regions). Thus we would have two separate refractive index gratings.

In addition, the self-lensing results [15] suggest that, initially, the positive Δn at the center of the illuminated region is larger than the positive Δn at the edge, whereas the positive Δn at the edge becomes much larger for longer write-times. This is in agreement with our previous requirement for the grating competition necessary to produce the observed FWM results. In light of this theory, we now suggest that the values for Δn reported earlier in this thesis are actually effective values. Moreover, the grating strength will now be referred to as the effective grating strength. Based on these ideas, we suggest the following process as the mechanism for permanent grating formation.

During permanent grating formation, the high-energy phonons produced by the non-radiative relaxation of Eu^{3+} ions provide the energy for modifier migration toward the dark regions. As the modifiers begin to migrate, a positive Δn is produced about the center of each illuminated region, and also in the regions of modifier buildup. Initially, however, the modifiers have not migrated far, and the concentration in the buildup region is not great enough to produce a comparable Δn. Therefore, the Δn in the center of each illuminated region forms an initially dominant grating that produces the increase in diffracted signal seen in the first few seconds of grating formation. As writing continues, the concentration of modifiers in the buildup region increases, and the buildup begins to enter the dark regions. Thus, a separate grating begins to form in the dark regions that interferes with the original grating to cause a decay in the diffracted power. Figures 22

(c)-(d) show the possible evolution of the gratings formed in the illuminated and dark regions [15]. As more modifiers migrate, the Δn in the dark regions becomes stronger than that in the illuminated regions. Thus, we see a minimum and subsequent increase in the diffracted power as a dominant grating forms in the dark regions. In Appendix I, we model our proposed dual refractive index gratings with dual multiple slit gratings to show how dual gratings could interfere to produce the change in diffracted power with time that was seen in the experiments.

As the grating formation temperature is lowered, the magnitude of the thermal vibrations of atoms in the glass network would become smaller. This would enable the modifiers to migrate through the interstices of the network more easily, and we would therefore expect a strong grating to form in the dark regions sooner at lower grating formation temperatures. Thus, the rate of decay after the initial maximum in diffracted power would be larger, and the minimum and subsequent increase in diffracted power would occur earlier in time at lower grating formation temperatures. We would also expect a stronger effective grating to form at a lower temperature due to the increased number of modifiers that could migrate to the dark regions. This is, in fact, what our experimental results have shown. In addition, if the grating in the dark regions formed more quickly at lower temperature, then, based on our model, we would expect the diffracted power at the initial maximum to be less at lower temperature since the interference effects would begin sooner. The initial maximum in diffracted power should also occur more quickly if the grating in the dark regions is forming more quickly. This is also what our experimental results have shown, as can be seen in Figure 16.
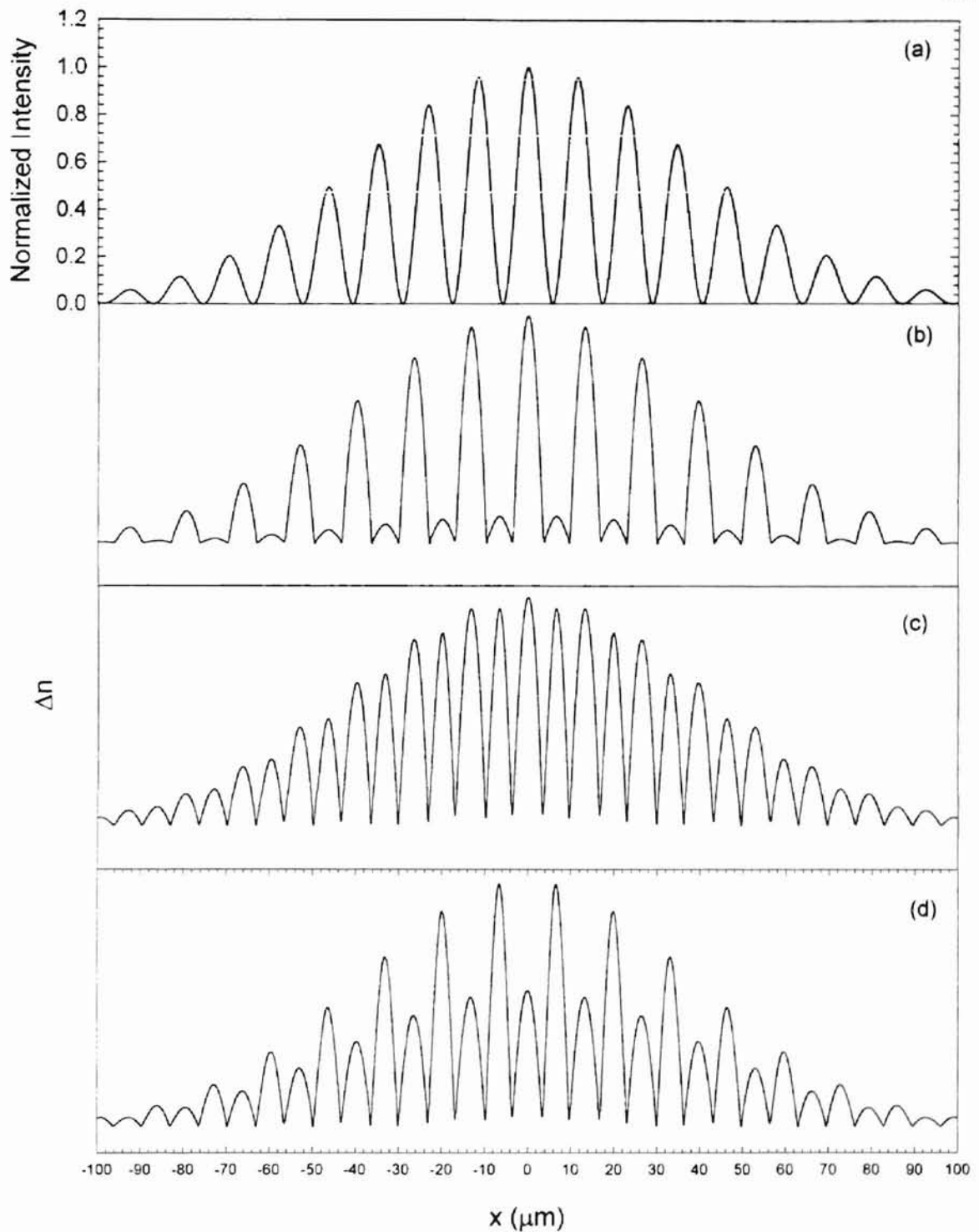
Figure 22 - (a) Normalized intensity pattern produced by two interfering gaussian beams. (b) - (d) show the possible Δn with time in the bright and dark regions of the interference pattern. Initially, as proposed, the grating in the dark regions is weak (b). As grating formation continues, the grating in the dark regions becomes similiar in magnitude, and then stronger than the Δn in the illuminated regions (C-D). Courtesy of Dr. A.Y. Hamad

This theory does have some limitations, however, as we do not notice a minimum in diffracted power during grating formation below room temperature in Eu2.5. Based on the ideas of dual grating formation stated above, we would expect to see a minimum in diffracted power in Eu2.5 if dual gratings were forming. It is likely that other processes are occurring in addition to the formation of dual gratings. Another possible contribution to the permanent grating is the effect of the electric fields that form between the regions where the modifiers migrate from and the build-up regions. If the modifiers migrate as positively charged ions, then the region where they build up would acquire a positive charge, and the region where they migrate from would acquire a negative charge. Thus, an electric field would be produced between these regions which would affect the polarizibility, and therefore the index of refraction. Taking this effect into account could help to explain why a minimum in diffracted power is not seen in Eu2.5 during grating formation below room temperature.

Grating Formation During Blocking

When the write-beams are turned off (block-period), there are no longer any hot phonons (from Eu^{3+} non-radiative relaxation) available for modifier migration. Thus, the theory above does not apply to the increase in grating strength during blocking since modifier migration can no longer be the cause. The strong increase in grating strength during blocking could possibly be due to a relaxation process occurring in the dark regions where there is an increased modifier concentration. The lack of an increase in diffracted power during blocking at room temperature in Eu5 could be explained by the

following: 1) the greater thermal energy at room temperature competes with the relaxation process. 2) At room temperature, the grating formed is not as strong, and therefore the concentration of modifiers in the dark regions is not as great. Thus the relaxation process, which is based on modifier concentration, would not be strong. Accordingly, we would expect the increase in grating strength during blocking to be greater for stronger gratings and at lower temperatures, which is exactly what was observed experimentally, as can be seen in Figure 15. Also, this explains why we see an increase in diffracted power at room temperature in Eu2.5 only when the grating at the time of blocking is strong. In addition, the results shown in Figures 18 and 19 can now be understood based on a relaxation process that is hindered by room temperature thermal energy: when the sample temperature is lowered, the relaxation process is able to occur, and we see an increase in diffracted power.

Since it is proposed that this relaxation process occurs when there is an increased modifier concentration, then we would expect it to occur during writing as well as blocking. However, its effect would be reduced during writing by the thermal energy produced by the laser write-beams. Thus when the write-beams are turned off, we would expect the relaxation process to produce a strong increase in diffracted power. The length of time over which this relaxation process occurred would be dependent on the modifier concentration, the temperature, and the exact nature of the relaxation process. For a stronger grating, the relaxation process should occur for a longer period of time. The relaxation process should also occur for a longer period of time at a lower temperature. This agrees with the results discussed in Chapter III. Although the exact

nature of the relaxation process is not known, the long periods of time over which it occurred (up to 42 hours) are typical for glasses.

CHAPTER V

CONCLUSION

Using the typical FWM technique, we studied the formation of superimposed permanent and transient LIG at and below room temperature in two Eu^{3+} doped silicate glasses. We were able to produce much stronger gratings below room temperature than at room temperature. In most cases, we found that during grating formation there was an initial maximum in diffracted power. followed by a minimum and subsequent increase. This was attributed to the formation of dual LIG in the sample. The LIG were proposed to be the result of modifier migration from the illuminated regions of the sample toward, and into the dark regions. A multiple-slit diffraction grating model was used to show how dual gratings could interfere to produce the change in diffracted power with time that was observed in these experiments. We also found that the grating strength increased during write-beam blockage. This was attributed to a relaxation process that occurred in the dark regions due to increased modifier concentration.

Further FWM studies should be conducted using more Eu^{3+} doped samples to determine if the grating formation trends described in this thesis persist at lower temperatures and with other Eu^{3+} concentrations. In addition, a careful study of grating formation verses write-beam crossing angle should be conducted. This will provide more information about the proposed dual grating formation since the write-beam interference

fringe spacing is determined by the write-beam crossing angle. In fact, a larger write-beam crossing angle will produce a smaller fringe spacing. Thus, the illuminated regions in the sample will be more closely spaced, and the modifiers would not have to migrate as far to reach the dark regions. Therefore, based on the dual grating theory, we would expect future FWM experiments to show a decrease in t_{min} as the write-beam-crossing angle is increased.

REFERENCES

[1]   F.M. Durville, E.G. Behrens, R.C. Powell, Physc. Rev. B 34 (1986) 4213

[2]   E.G. Behrens, F.M. Durville, R.C. Powell, Opt. Lett. 11 (1986) 653

[3]   E.G. Behrens, F.M. Durville, R.C. Powell, Physc. Rev. B 39 (1989) 6076

[4]   E.G. Behrens, R.C. Powell, J. Opt. Soc. Am. B 7 (1990) 1437

[5]   V.A. French, R.C. Powell, D.H. Blackburn, D.C. Cranmer, J. Appl. Physc. 69 (1991) 913

[6]   M.M. Broer, A.J. Bruce, W.H. Grodkiewicz, J. Lumin. 53 (1992) 15

[7]   M.M. Broer, A.J. Bruce, W.H. Grodkiewicz, Phys. Rev. B 45 (1992) 7077

[8]   A. Munoz, R.J. Reeves, B. Taheri, R.C. Powell, J. Chem. Phys. 98 (1993) 6083

[9]   A.Y. Hamad, J.P. Wicksted, G.S. Dixon, L.P. deRochemont, J. Non-Cryst. Solids 241 (1998) 59

[10]   A.Y. Hamad, J.P. Wicksted, G.S. Dixon, Opt. Mat. 12 (1999) 41

[11]   G.S. Dixon, A.Y. Hamad, J.P. Wicksted, Phys. Rev. B 58 (1998) 200

[12]   S.M. Mian, A.Y. Hamad, J.P. Wicksted, Appl. Opt. 35 (1996) 6825

[13]   A.Y. Hamad, J.P. Wicksted, Opt. Commun. 138 (1997) 354

[14]   G.S. Dixon, private communication

[15]   A.Y. Hamad, unpublished work

[16]   E. Hecht, Optics (Addison-Wesley, Reading, MA, 1987), 409-410.

Appendix I

To show how dual gratings could interfere to produce the change in diffracted power with time that was observed in our experiments, we use a multiple-slit diffraction grating model. Assuming plane waves at normal incidence, the diffracted electric field from a single multiple-slit grating, G_1, with slit width b, and center to center spacing a is

$$E_1 = bC(\sin\beta/\beta)(\sin N\alpha/\sin\alpha)(\sin[\omega t - \kappa R + (N-1)\alpha]), \qquad (1)$$

where $\beta = (\kappa b/2)\sin\theta$, $\alpha = (\kappa a/2)\sin\theta$, C is a factor that corresponds to the strength of the grating, N is the number of slits, R is the magnitude of the vector from the origin to the point of observation, θ is the angle of the vector R, and ω and κ are the frequency and wave vector of the incident plane wave [16]. The intensity of E_1 is found by taking the time average of $(E_1)^2$. This gives

$$I_1(\theta) = (1/2)(bC)^2(\sin\beta/\beta)^2(\sin N\alpha/\sin\alpha)^2. \qquad (2)$$

We can model the interference of two gratings by considering a second multiple slit grating, G_2, that forms in-between the slits of G_1. We consider the case where the slit width of G_2 is half that of G_1, and the slit spacing is the same. Also, we consider the case where G_2 is exactly out of phase with G_1. This produces the effective grating G_{12} from which we can calculate the electric field produced by the interference of G_1 and G_2. Again, assuming plane waves at normal incidence, the diffracted electric field from G_{12} is

$$E_{12} = bC(\sin\beta/\beta)(\sin N\alpha/\sin\alpha)(\sin[\omega t - \kappa R + (N-1)\alpha])$$
$$+ (bD/2)(\sin(\beta/2)/(\beta/2)) (\sin N\alpha/\sin\alpha)(\sin[\omega t - \kappa R + N\alpha]), \qquad (3)$$

where D is a factor that corresponds to the different grating strength of G_2. Again, we

calculate the intensity of E_{12} by taking the time average of $(E_{12})^2$. This gives

$$I_{12}(\theta) = (1/2)(bC)^2(\sin\beta/\beta)^2(\sin N\alpha/\sin\alpha)^2$$
$$+ (1/2)(bD/2)^2(\sin(\beta/2)/(\beta/2))^2(\sin N\alpha/\sin\alpha)^2$$
$$+ (bC)(bD/2)(\sin\beta/\beta)(\sin(\beta/2)/(\beta/2))(\sin N\alpha/\sin\alpha)^2(\cos\alpha/2). \qquad (4)$$

We can now compare I_1 with I_{12} to show that interference between G_1 and G_2

does in fact take place to produce a minimum in the diffracted signal. Figure 23 shows I_1

and I_{12} as a function of θ for b = 3μm, a = 7μm, C = 0.2, D = 0.1, λ = 465.8nm, N = 30,

and R = 1m. These parameters closely parallel our experimental conditions. The choice

of C ~ D was made to simulate gratings of similar strength, however, the values chosen

were completely arbitrary. As can be seen, at the first order fringe, the interference of G_1

and G_2 produces less diffracted intensity than G_1 alone produces. Thus we see that

interfering gratings of similar strength can produce a minimum in diffracted signal.

By adjusting C and D, we can change the relative strengths of G_1 and G_2, and

simulate the effective grating at a given time. Initially, we expect that G_1 is strong, and

G_2 is weak so that we have essentially one dominant grating. After long write-times, we

expect that G_2 becomes much stronger than G_1 so that we again have one dominant

grating. Figure 24 shows the diffracted signal from G_{12} for three different choices of D.

As can be seen, when C > D, we have a strong diffracted signal, when C ~ D, the

diffracted signal is much weaker, and when D > C, we again get a strong diffracted

signal. This simulates an initial maximum in diffracted power followed by a minimum

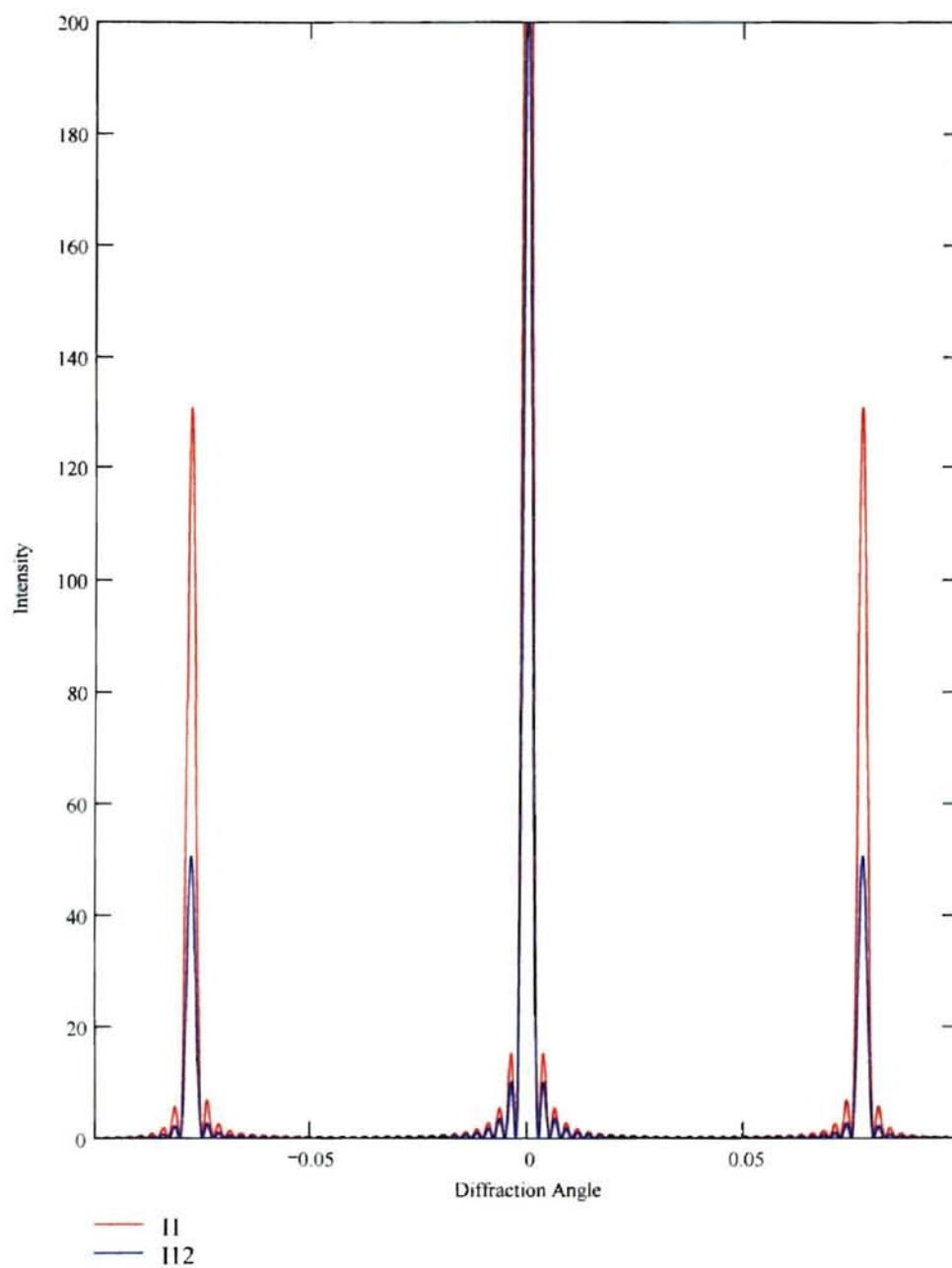and subsequent increase, and closely parallels what was experimentally observed.

Figure 23 - Calculated diffraction intensity for a single grating, (red) and
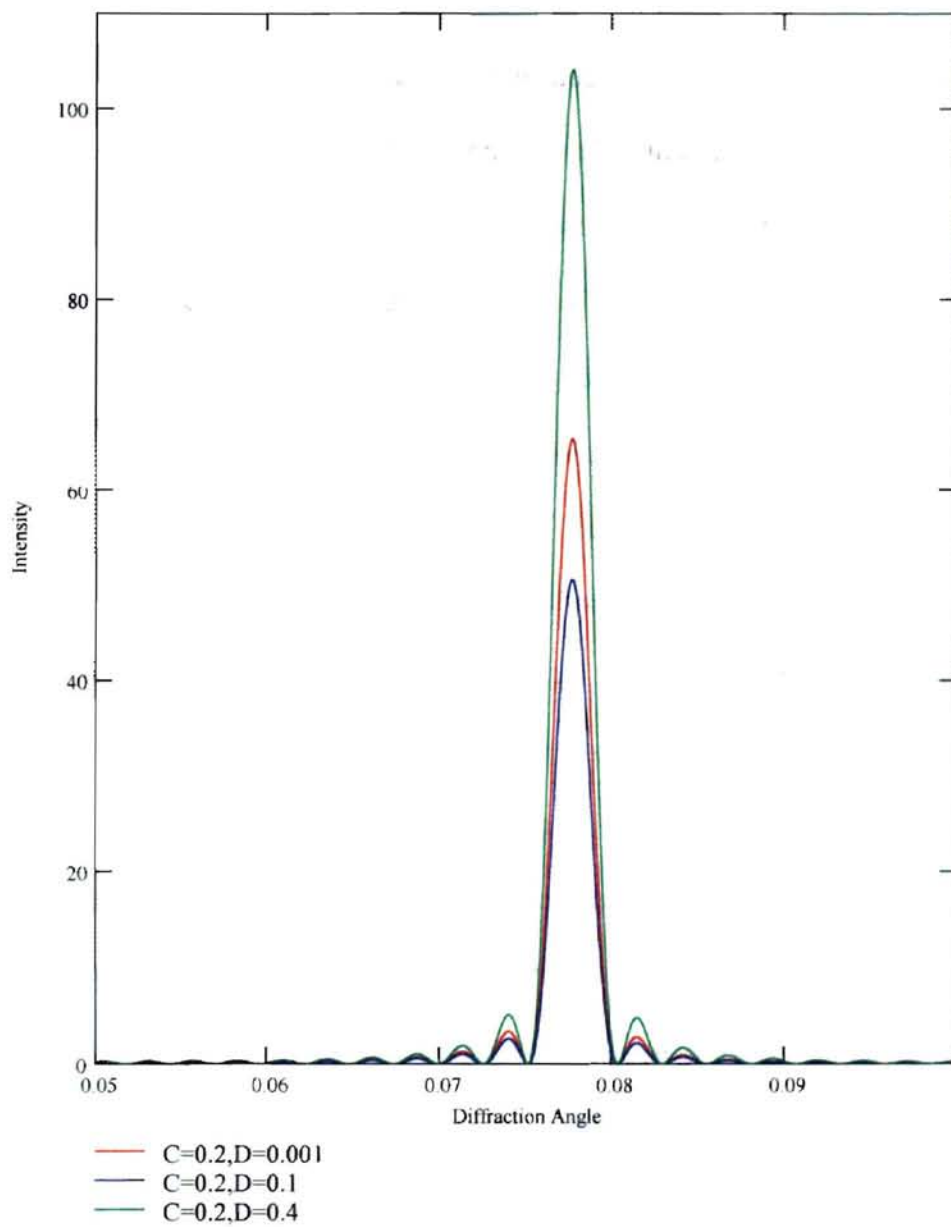dual gratings (blue) using equations (2) and (4) respectively.

Figure 24 - Calculated intensity for two interfering multiple-slit gratings from eq. (4). Each calculation is for a different set of grating strengths. Only shown is the first-order diffraction region.

Appendix II

The purpose of this appendix is to quantify the differences between the growth and decay of gratings formed in different samples and under different conditions. To do this we will give the results of some mathematical fits to our experimental data. The fits were made to the non-linear change in index of refraction, Δn.

The regions of interest during the grating formation process in Eu5 were the decay in grating strength after the initial maximum, and the increase in grating strength after the minimum. In Eu2.5, the region of interest was the increase in grating strength after the initial "jump". For simplicity in discussing the fits in this appendix, we will refer to these regions as the growth and decay regions of Eu5, and the growth region of Eu2.5. The regions of initial increase in grating strength were not fit for either sample. In addition, only the regions corresponding to the writing of the grating were fit. The regions corresponding to an increase in grating strength during blocking were not fit. Furthermore, all data that were fit correspond to a write-beam power of 50mW.

At 238K, Δn in the growth region of Eu2.5 was found to increase nearly linearly with time for shorter write-times (approximately up to 1 hour). The important parameter describing this linear increase in Δn is the slope, and for Eu2.5 at 238K, we found the slope to be $(1.543\pm0.287)\times10^{-7}$. For longer times (greater than 1 hour), Δn in the growth region of Eu2.5 was seen to begin to limit, and was fit well with a second order function $(\Delta n = \Delta n_0 + \Delta n_1 t + \Delta n_2 t^2)$, where we found Δn_1 to be $(1.908\pm0.149)\times10^{-7}$ and Δn_2 to be

$(-3.565\pm0.205)\times10^{-10}$. In Eu5 at 238K and 265K, Δn in the growth region was found to initially increase parabolically with time, and was fit well with a second-order function. At 238K we found Δn_1 to be $(3.36\pm3.10)\times10^{-8}$ and Δn_2 to be $(4.589\pm0.895)\times10^{-10}$, and at 265K we found Δn_1 to be $(-6.16\pm4.60)\times10^{-9}$ and Δn_2 to be $(1.163\pm1.087)\times10^{-10}$. After this parabolic increase, Δn in the growth region of Eu5 at 238K and 265K was seen to increase nearly linearly with time. We found the slope at 238K to be $(8.75\pm1.56)\times10^{-8}$, and the slope at 265K to be $(2.85\pm0.87)\times10^{-8}$. In the growth region of Eu5 at room temperature, Δn increased linearly in time with slope $(0.74\pm0.42)\times10^{-8}$. The Δn in the decay region of Eu5 was found to fall off exponentially with time at all temperatures, and was fit well with a three-parameter exponential function ($\Delta n = \Delta n_0 + \Delta n_1\exp[\Delta n_2 t]$). The important parameter describing the decay is Δn_2. The values for Δn_2 were found to be -0.55 ± 0.03, -0.43 ± 0.02, and -0.32 ± 0.02 for 238K, 265K, and 298K respectively.

As an example, we show a fit to the growth region of Eu2.5 for grating formation at 238K. As can be seen in Figure 25, the data corresponding to the first hour of grating formation are fit well with a linear function. To make this fit, the data corresponding to the initial "jump" in grating strength (approximately the first 3 minutes) were removed from the plot. The remaining data were then fit with the function shown using Sigma Plot software. All other fits were made in a similar fashion.
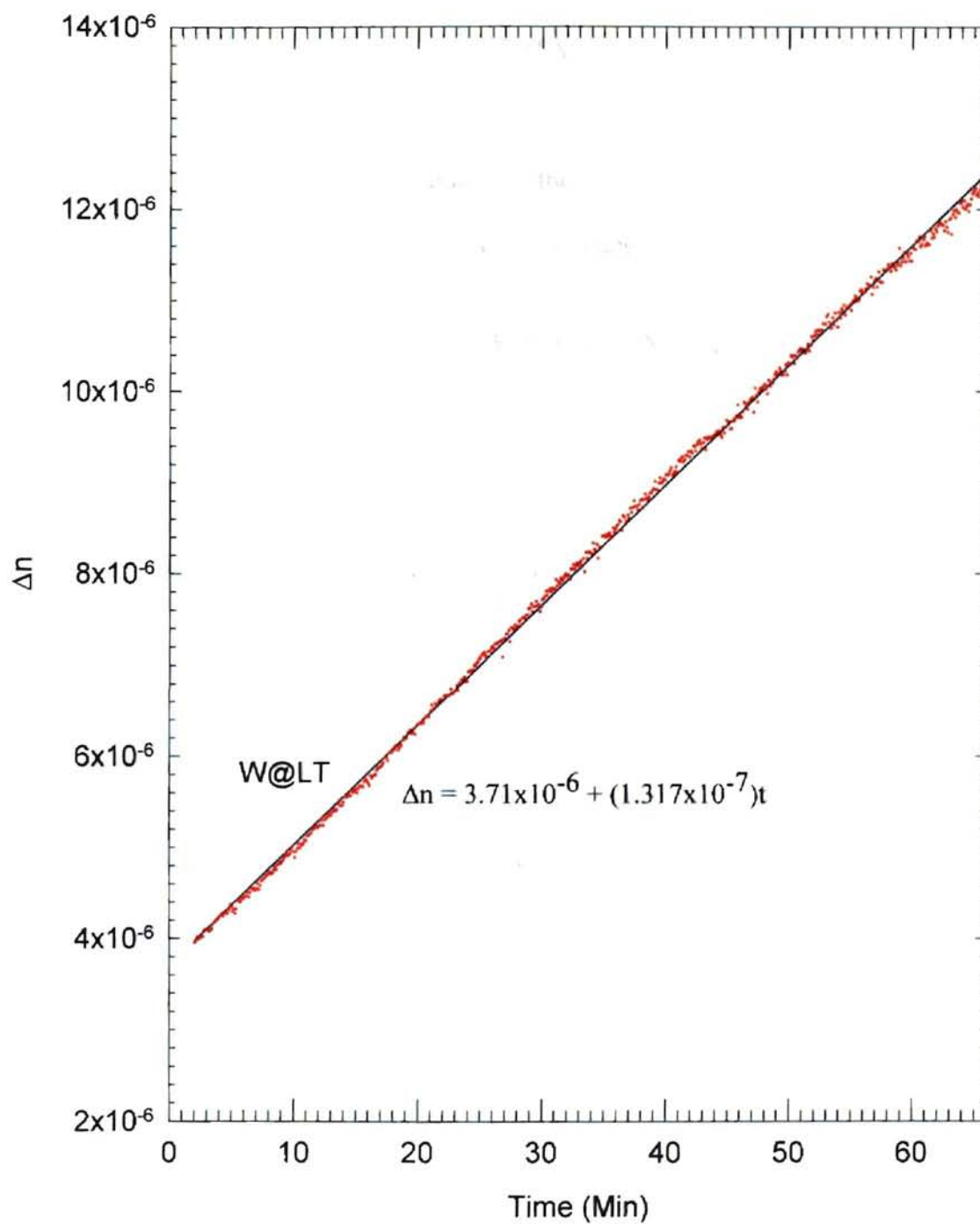
Figure 25 - Mathematical fit of data corresponding to grating formation in Eu2.5 at 238K for a write-beam power of 50mW.

VITA

Jason Paxton

Candidate for the Degree of

Master of Science

Thesis: FOUR-WAVE MIXING BELOW ROOM TEMPERATURE IN EU^{3+} DOPED SILICATE GLASSES

Major Field: Physics

Biographical:

Education: Graduated from Putnam City North High School, Oklahoma City, Oklahoma in May 1993; received Bachelor of Science degree in Physics from the University of Central Oklahoma, Edmond, Oklahoma in August 1997. Completed the requirements for the Master of Science degree with a major in Physics at Oklahoma State University, Stillwater, Oklahoma in July 1999.

Experience: Employed by the University of Central Oklahoma as a teaching assistant from 1995 to 1997; employed by Oklahoma State University as a teaching assistant from 1997 to 1998; employed by Oklahoma State University as a research assistant from 1998 to present.

Professional Memberships: Sigma Pi Sigma, American Physical Society.